



Faculty of Science and Technology

## MASTER'S THESIS

Study program/Specialization: Petroleum Engineering / Well Engineering	Spring semester, 2016  <del>Open</del> / Restricted access
Writer: Hafiz Adi Kurnia	..... (Writer's signature)
Faculty supervisor: Dan Sui  External supervisor(s):	
Thesis title: Adaptive Observer Design for Linear Hyperbolic System in Managed Pressure Drilling	
Credits (ECTS): 30	
Key words: Adaptive Observer Managed Pressure Drilling Drilling Automation	Pages: 77  + enclosure: 6  Stavanger, June 2016



**Master Thesis**  
**PETMAS**

Adaptive Observer Design for Linear Hyperbolic System  
in Managed Pressure Drilling



Universitetet  
i Stavanger

---

Hafiz Adi Kurnia

**University of Stavanger**

# ABSTRACT

Managed Pressure Drilling (MPD) is a drilling technology that has been developed to manage and control the downhole pressure in the well in order to minimize drilling-related problems. This technology uses a pressurized closed-loop system and specialized equipment that allows better and more accurate pressure control of downhole pressure profile, therefore avoids drilling problems associated with downhole pressure variations, optimizes the drilling process by minimizing the non-productive time (NPT) and enables drilling prospects that are technically and/or economically un-drillable with conventional drilling methods.

An essential part of Managed Pressure Drilling operation is the control of the downhole pressure and it can be a challenging task due to the complex dynamics of wellbore hydraulics. In order to estimate the downhole pressure profile, a simplified hydraulic model has been recognized as a more convenient alternative than advanced hydraulic model since in the most cases, the available data contain insufficient information and several parameters are both uncertain and slowly changing that leads to higher level of complexity for the advanced hydraulic model.

By using simplified hydraulic model and available measurements, the pressure and flow dynamics of the well can be estimated. However, the downhole measurement is less reliable than the topside measurement because of slow sampling, and loss of communication for low or no-flow conditions, e.g., during pipe connection procedures. Depending just on the topside measurement, the downhole pressure needs to be accurately estimated despite the uncertainties in parameters such as friction, density, fluid loss etc.

This Master Thesis work describes an adaptive observer design to estimate the system states and the unknown parameter for the hydraulics of Managed Pressure Drilling using only one boundary measurement at the topside. Numerical simulations are performed to demonstrate the effectiveness of the adaptive observer. The results from simulations of drilling events such as drilling connection and lost circulation and also analysis from Lyapunov approach shows that the estimation error converges to zero, and the downhole pressure, the flow dynamics, the rate of lost circulation and other unknown parameters can be accurately estimated.

## **ACKNOWLEDGEMENTS**

This thesis is submitted as partial fulfillment for the requirements of Master of Science (M.Sc.) at the University of Stavanger (UiS), Norway. It would not have been possible to complete this thesis without assistance, support, guidance, and help from many individuals.

I would like to thank Prof. Dan Sui for the patient guidance, encouragement, and all the good discussions we have had for this thesis. I have been fortunate to have her as my supervisor who always respond to all my queries so promptly. Without her support and guidance during my thesis writing, I would not be able to complete it on time.

I would like to thank Mas Agus Hasan who introduced me to the adaptive observer design and gave me ideas, suggestion and always try his best to answer all of my questions during my thesis writing.

I want to thank my parents, for their continuous support, motivation and encouragement in everything I did. Last but not least, thank you to my fellow Indonesians in Stavanger and a great friend of mine, Samuel Erzuah, for the joy that we have had during our stay in Stavanger.

Hafiz Adi Kurnia

# TABLE OF CONTENTS

ABSTRACT .....	I
ACKNOWLEDGEMENTS.....	II
TABLE OF CONTENTS.....	III
LIST OF FIGURES .....	V
LIST OF TABLES .....	VI
1. INTRODUCTION .....	1
1.1 Background .....	1
1.2 Objective.....	4
1.3 Thesis outline .....	4
2. THEORETICAL BACKGROUND.....	5
2.1 Managed Pressure Drilling .....	5
2.1.1 Definition.....	6
2.1.2 Pressure Control in MPD .....	7
2.1.3 Benefits of MPD.....	11
2.1.4 MPD Techniques and Tools.....	13
2.2 Pressure Estimation in Managed Pressure Drilling.....	20
2.2.1 Adaptive Observer.....	21
3. HYDRAULIC WELL MODEL.....	24
3.1 Fit for Purpose Modelling.....	24
3.2 Outline of Model Derivation.....	26
3.2.1 Equation of State .....	27
3.2.2 Equation of Continuity .....	28
3.2.3 Equation of Momentum .....	29
3.3 Simplified Hydraulic Model .....	31
3.3.1 Simplified ODE Model .....	31
3.3.2 Simplified PDE Model.....	33
4. TRANSFORMATION OF HYDRAULIC MODEL.....	36
4.1 Model Transformation .....	36

4.2	Discretization.....	40
4.3	Simulation .....	43
5.	ADAPTIVE OBSERVER DESIGN .....	48
5.1	State and Parameter Estimation .....	49
5.1.1	Adaptive Observer.....	49
5.1.2	Error Dynamics.....	50
5.1.3	Lyapunov Analysis.....	51
5.2	Error Dynamics .....	51
5.3	Convergence of Estimated State ( $\omega$ ) and Parameter ( $\theta$ ).....	55
5.4	Simulation .....	55
6.	CONCLUSION AND FUTURE WORK .....	63
6.1	Conclusion.....	63
6.2	Future Work .....	63
	REFERENCE .....	65
	NOMENCLATURE .....	68
	APPENDIX A .....	71
	APPENDIX B .....	74

## LIST OF FIGURES

Figure 2.1: Illustration of Automated Managed Pressure Drilling System.....	8
Figure 2.2: Pressure Window and Pressure Profile for UBD, MPD and OBD.....	9
Figure 2.3: Pressure Profile in Conventional Drilling Operation.....	10
Figure 2.4: Pressure Profile in Managed Pressure Drilling Operation.....	11
Figure 2.5: Normal Operational Window.....	11
Figure 2.6: Narrow Operational Window.....	12
Figure 2.7: Pressure Profile in Constant Bottomhole Pressure.....	14
Figure 2.8: Pressure Profile in Pressurized Mud Cap Drilling.....	14
Figure 2.9: Pressure Profile in Dual Gradient Drilling.....	15
Figure 2.10: Schematic of Riserless Drilling.....	16
Figure 2.11: Rotating Control Device.....	17
Figure 2.12: Operation Principle of Semi Auto Choke.....	18
Figure 2.13: Non-Return Valves.....	19
Figure 2.14: Coriolis Flowmeter.....	19
Figure 2.16: MPD Multiphase Separation System.....	20
Figure 3.1: Simplified Schematic of the Drillstring and Annulus.....	31
Figure 4.1: Schematic of Managed Pressure Drilling System. ....	37
Figure 4.2: Flowrate at the Inlet (Bottomhole).....	44
Figure 4.3: Flowrate at the Outlet (Choke).....	45
Figure 4.4: Pressure at the Inlet (Bottomhole).....	46
Figure 4.5: Pressure at the Outlet (Choke).....	47
Figure 5.1: Flowrate at the Inlet (Bottomhole).....	57
Figure 5.2: Flowrate at the Outlet (Choke).....	58
Figure 5.3: Pressure at the Inlet (Bottomhole).....	58
Figure 5.4: Pressure at the Outlet (Choke).....	59
Figure 5.5: Flowrate at the Outlet (Choke).....	61
Figure 5.6: Pressure at the Inlet (Bottomhole).....	61
Figure 5.7: Fluid Loss Estimation.....	62



## LIST OF TABLES

Table 4.1: Wellbore Parameters for Simulation of Drilling Connection .....	43
Table 5.1: Wellbore Parameters for Simulation of Loss Circulation.....	60

# 1. INTRODUCTION

## 1.1 BACKGROUND

The increase in the energy consumption rates that leads to the continuing high demands for petroleum and energy worldwide drives the oil and gas industry to discover ways to recover the resources that have been already used for years. However, the remaining prospect for hydrocarbon resources typically will be more challenging to drill compared to the past. One of the main challenges drilling these new prospects is related to drill wells with narrow pressure margin, e.g., drilling into depleted reservoirs or drilling wells with the shallow onset of abnormal pressure. In addition, safety and efficient drilling are very important issues to keep in mind for drilling operation and it leads into increasing requirement to the technology in the drilling industry.

Managed Pressure Drilling (MPD) is a technology that addresses many of drilling-related issues or barriers to conventional drilling methods. This technology utilizes both a pressurized closed-loop drilling system and specialized equipment to more precisely control the downhole pressure profile throughout the wellbore (Hannegan, 2006). This is accomplished by sealing the top drive with a rotating control device (RCD), the use of a control valve and an extra pump. The aim is to maintain the downhole pressure profile within the pressure zone (formation pressure, collapse pressure, and fracture pressure) that is often referred to as pressure window.

The pressurized closed-loop drilling system allows better and more accurate control of downhole pressure profile, therefore avoiding drilling problems associated with downhole pressure variation, optimizing the drilling process by minimizing the non-productive time (NPT) and enabling drilling prospects that are technically and/or economically un-drillable with conventional drilling methods (Rehm et al, 2008).

In order to have an accurate pressure control in MPD operation, not only the mechanics of this pressurized closed-loop system or the software that need to be developed, but the entire MPD system needs to be designed from a control system point of view. Automation in MPD operation relates to the control system that regulates the choke opening at the topside facility in order to maintain the downhole pressure during any drilling events such as connection and loss circulation.

This automated MPD system requires a hydraulic well model that estimates the downhole pressure and a feedback control that automatically regulate the choke opening to maintain the required choke pressure according to the set point. Hence, the hydraulic well model plays an important role in determining the accuracy of the MPD system.

In order to estimate the downhole pressure profile, some advanced hydraulic model has been developed to capture some particular aspects of drilling that is useful to compute some specific events or problems during the drilling operation. However, in most cases, the available data contain insufficient information required for an advanced hydraulic model. In addition, several parameters such as friction coefficient throughout the wellbore and the influx or outflux (loss circulation) rate are both uncertain and slowly changing. As this work aim to identify the hydraulic of MPD system, the mathematical model is not supposed to be too complex, since an advanced model requires a high number of measurement and adjustment of drilling parameter during operation and it would not be able to present a proper parameter estimation scheme (Kaasa et al, 2011). A simplified hydraulic model that captures the dominant phenomena of the drilling system has been recognized as a more convenient alternative than the advanced hydraulic model.

Using the simplified hydraulic model and data from the available measurements, the downhole pressure can be estimated. However, the downhole measurement is less reliable than the topside measurement because the sensors are expensive, the data obtained are often noisy, and also due to slow sampling, and loss of communication for low or no-flow conditions, e.g., during pipe connection procedures. Therefore, the topside measurement will act as a control input in order to estimate the downhole pressure. The pressure profile can be difficult to obtain as it is a complex function of drilling parameters such as friction, density, etc. and these values have high degrees of uncertainty as there is no direct way of measuring them. Therefore, the downhole pressure has to be estimated and uncertainties should be taken into account when doing so. Depending just on the topside measurement, the downhole pressure needs to be accurately estimated despite the uncertainties in parameters such as friction, density, fluid loss etc. (Stamnes, 2011).

For the estimation of the bottom hole pressure, the hydraulic system in MPD operation can be modeled by linear  $2 \times 2$  partial differential equations (PDEs) of hyperbolic type. This type hyperbolic PDEs has attracted considerable attention due to the many examples of fluid flow systems that can

be modelled that way, such as flow of fluids in transmission lines (Curro, Fusco, and Mangarano, 2011), gas flow pipelines (Gugat and Dick, 2011), mud flow in oil well drilling (Kaasa, 2012; Hauge, 2013; Hasan, 2014). The estimation of the dynamic system using deterministic approach is called as an observer. An observer is mainly used to estimate the dynamic system while the parameters are well-known. On the other hand, an adaptive observer is useful in the case of uncertain parameters in the system. As in the case of MPD operation, there are uncertain parameters such as friction, influx and fluid loss that need to be accurately estimated in order to have an accurate estimation of the state system, that is pressure dynamics of the wellbore.

As the hydraulic model is transformed into  $2 \times 2$  linear hyperbolic system PDEs, then the adaptive observer for this specific class of linear hyperbolic system needs to be reviewed. In this work, the adaptive observer is presented based on a backstepping method that is a systematic method for control and estimation problems of distributed parameter systems that have been used successfully for state and parameter estimation of many types of PDEs. This backstepping method allows the design of boundary control laws, boundary observers and output-feedback control laws, which guarantee the stability of the closed-loop system and convergence of the state estimates. The design, which is based on Volterra integral transformation relies only on a measurement at the right boundary of the system (topside), and the observer gains are obtained by solving a first-order hyperbolic system of Goursat-type PDEs (Hasan et al, 2015). This solution to the Goursat system is related to the solution of a simpler, explicitly solvable Goursat system through a suitable infinite series of powers of partial derivatives which is summed explicitly in terms of special functions, such as Bessel functions and the generalized Marcum Q-functions of the first order (Vazquez et al, 2013).

This Master Thesis work describes an adaptive observer design to estimate the system states and the unknown parameter for the hydraulics of Managed Pressure Drilling using only one boundary measurement at the top of the well. Using an adaptive observer, where an uncertain parameter is estimated using the update-law, the downhole pressure and the rate of lost circulation can be accurately estimated and numerical simulations are performed to demonstrate the effectiveness of the adaptive observer.

## **1.2 OBJECTIVE**

The main goal of this thesis is to:

1. Present Adaptive Observer Design for estimation of states and unknown parameters using only one measurement at the boundary (top of the well) in MPD operations.
2. Present the proof of stability of Lyapunov-based adaptive observer to show that the estimates converge exponentially to the actual values.
3. Perform a simulation study for drilling connection and lost circulation.

## **1.3 THESIS OUTLINE**

The thesis is divided into 4 parts, and organized as follow:

1. Part 1 (Chapter 1 - 2) provides an introduction, motivation, objective and presents necessary background on the technology evaluated and used in this thesis, managed pressure drilling, and the idea behind the pressure estimation in a drilling operation and adaptive observer design.
2. Part 2 (Chapter 3 – 4) presents the mathematical model of the wellbore hydraulics, its transformation, and discretization. This part is introduced by the fit for purpose of modelling, derivation of generic low-order expression for pressure and flow dynamics, and proceeds with the model transformation.
3. Part 3 (Chapter 5) is the main part of thesis, with presentation and detailed derivations of adaptive observer for the hyperbolic system, prove of convergence of the proposed scheme and analysis and discussion of the simulation results.
4. Part 4 (Chapter 6) summarizes the results from this thesis and presents the conclusion.

## **2. THEORETICAL BACKGROUND**

As an introductory review for pressure control in Managed Pressure Drilling, this chapter presents the necessary background to understand the concept of MPD and downhole pressure estimation with an adaptive observer. This chapter summarizes the relevant information from the review of the literature on MPD operations and downhole pressure estimation. It provides an overview of MPD concepts compared to conventional drilling, its definition, application and benefits and also the different approach and equipment being used in MPD operation. For downhole pressure estimation, this chapter provides the necessary background on the need for accurate pressure estimation and the use of adaptive observer to estimate the MPD system states and unknown parameters.

### **2.1 MANAGED PRESSURE DRILLING**

In today's drilling environment, the industry is facing a greater challenge to drill the remaining prospect of hydrocarbon. One of the main challenges drilling these new prospects is related to drill wells with narrow pressure margin, e.g., drilling into depleted reservoirs or drilling wells with the shallow onset of abnormal pressure. Drilling into an area with the formation pressure very close to the fracture pressure will likely lead into drilling issues such as kick, loss circulation, stuck pipe etc. In addition, safety and efficient drilling are very important issues to keep in mind for a drilling operation. Due to these reasons, there are certain needs for increasing the requirement to the technology in the drilling industry.

Managed Pressure Drilling (MPD) is an enabling technology that can help to accomplish those needs by addressing many of drilling-related issues or barriers to conventional drilling methods. This technology utilizes both a pressurized closed-loop drilling system and specialized equipment to more precisely control the downhole pressure profile throughout the wellbore (Hannegan, 2006). The aim is to maintain the downhole pressure profile within the pressure zone (formation pressure, collapse pressure, and fracture pressure) that is often referred to as pressure window.

By having a better and more accurate control of downhole pressure profile using this pressurized closed-loop system, MPD helps to reduce non-productive time (NPT) and avoid many drilling-

related issues such as kick, lost circulation, wellbore stability, stuck pipe, ballooning, potential damage to the reservoir, low rate of penetration (ROP), excessive mud cost due to the lost circulation, excessive number of casing string, failure to reach TD with proper hole diameter, and shallow geohazard etc (Rehm et al, 2008; Nas et al, 2009). With all the benefits and the capability to drill what was considered economically un-drillable wells, Managed Pressure Drilling has gained widespread popularity and a great deal of press coverage in the last decade.

This section provides a closer look at what this really means, and what can be gained by using MPD rather than conventional drilling methods.

### **2.1.1 Definition**

Managed Pressure Drilling, according to the International Association of Drilling Contractors (IADC), is defined as *“an adaptive drilling process used to more precisely control the annular pressure profile throughout the wellbore”*. *The objectives are to ascertain the downhole pressure environment limits and to manage the annular hydraulic pressure profile accordingly.*” (IADC; Hannegan, 2005).

Further, MPD can be defined as (IADC; Hannegan, 2005):

- MPD process employs a collection of tools and techniques which may mitigate the risks and costs associated with drilling wells that have narrow downhole environmental limits, by proactively managing the annular hydraulic pressure profile.
- MPD may include control of backpressure, fluid density, fluid rheology, annular fluid level, circulating friction, and hole geometry, or combinations thereof.
- MPD may allow a faster corrective action to deal with observed pressure variations. The ability to dynamically control annular pressures facilitates drilling of what might otherwise be economically unattainable prospects.

IADC also separate MPD into two categories:

- Reactive MPD: The well is drilled using conventional drilling method and as soon as unexpected pressure arise, the equipment for MPD system is rigged up to quickly react to the unexpected pressure changes.

- Proactive MPD: The drilling program is designed to take full advantage of the ability to precisely managed the downhole pressure profile, often referred as ‘walk the line’. This category offers the greatest benefit of MPD operation, but it requires the well to be pre-planned more thoroughly.

### **2.1.2 Pressure Control in MPD**

In a drilling operation including MPD as illustrated in Figure 2.1, the topdrive which is a motor that turns the drillstring transmit the torque via the drillstring into the bit. The rotation of the drill bit at the bottom of the wellbore will remove or cut the formation in order to create holes or known as the wellbore. As a result, it generates drill cuttings which are a broken solid material removed from a formation. These cuttings have to be circulated out of the wellbore to avoid the cutting deposit in the bottomhole that might disrupt the drilling process. Once the bit on the bottom has drilled down to where the topdrive at the top reach the drillfloor, approximately 90ft, a new stand of pipe is again connected to the topdrive. This procedure is known as drilling connection. In addition to transmitting the torque to the bit, the drillstring also transmit the drilling fluid from the rig pumps through the drilling, the drill bit and up to the surface. The drilling fluid from the mud pit will be transferred to the rig pump, which pumps down a viscous drilling mud through the top drive, the drillstring, and the drill bit. The viscous drilling mud from the drillstring flows through the bit and carry the cutting into the annulus and the surface. The circulation of the drilling fluid is an important part of drilling operation because not only it will remove the cutting from the wellbore, the column of the drilling fluid along the wellbore provides hydrostatic pressure against the high-pressure formation.



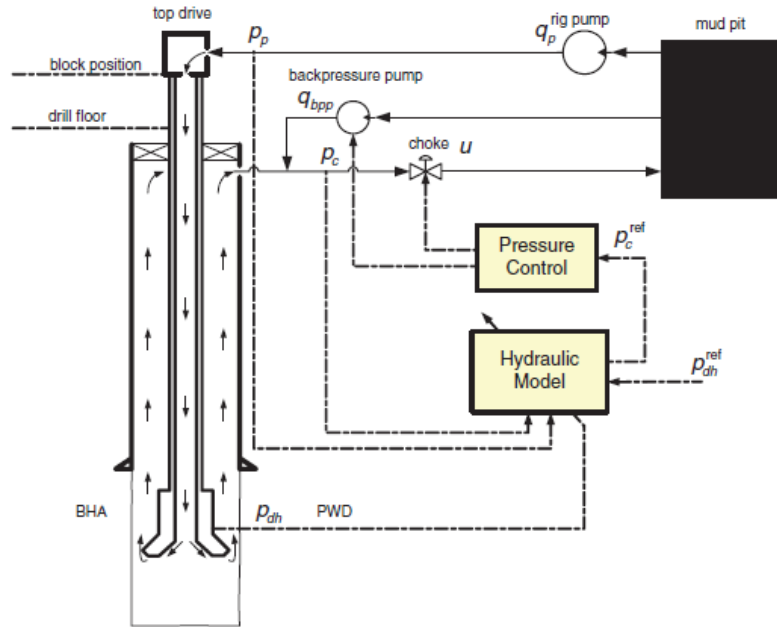


**Figure 2.1: Illustration of Automated Managed Pressure Drilling System (Kaasa, 2008)**

The downhole pressure needs to be maintained within the pore pressure, fracture pressure, and collapse pressure or often referred as pressure window. Pore pressure is the pressure exerted by formation fluid within the pores space of rock as a result of the overburden formation and fluids above. If the downhole pressure is less than the pore pressure, there will be an influx of formation fluids or hydrocarbon into the wellbore or known as a kick. A large amount of influx and an uncontrolled kick might lead into a blowout, which has catastrophic consequences for life and environment. Even if the effective measure can be taken to handle the kick, circulating the high-pressure kick out of the wellbore might lead into wellbore collapse and stuck pipe.

The upper-pressure limit for the downhole pressure is the fracture pressure, which is the minimum pressure that will fracture the formation. If the downhole pressure exceeds the fracture pressure, there will be a fracture opening that leads into lost circulation or formation damage. On the other hand, if downhole pressure is lower than the collapse pressure, it might reduce the structural integrity of the wellbore and cause pipe sticking or well collapse (Azar & Samuel, 2007).

The uncertainties in pore pressure, fracture pressure and collapse pressure due to the geological unknowns and maturing fields also lead into difficulties to understand the pressure regime in which the drilling operation takes place. In the exploration for the new prospect, there are geological

uncertainties such as depth correlation or seismic time and the effect it has on pore pressure model. Meanwhile in mature fields, as a result of the reservoir being drawn down, the in-situ stress are redistributed and later create a narrow pressure window. Ensuring that the downhole pressure stays within the pressure window is essential to ensure safe as well as economically sound drilling operations.

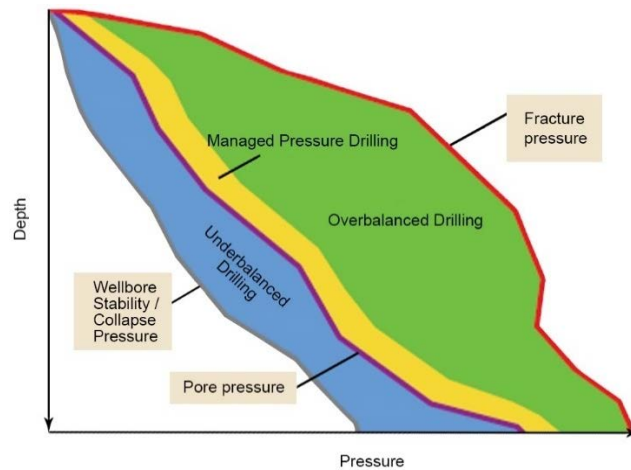


**Figure 2.2: Pressure Window and Pressure Profile for UBD, MPD and OBD.  
Redrawn from Schlumberger (2011)**

In conventional drilling, the bottomhole pressure is equal to the sum of the hydrostatic weight of the mud column and the frictional pressure along the annulus, known as equivalent circulating density (ECD). The frictional pressure is a result of mud circulation in the wellbore while drilling the formation. However, in some specific cases or part of drilling procedure e.g., drilling connection, the mud circulation will be stopped at some point and it leads to loss of annular frictional pressure (AFP). As a result of the loss of annular frictional pressure, the bottom hole pressure in Eq. (2.1) will be equal to the hydrostatic pressure of the mud column or called as equivalent static density (ESD). While drilling operation takes place in a formation with normal pressure window, the loss of AFP might still keep the bottomhole pressure within the safe pressure window. However, challenging drilling environment such as depleted reservoir and the deepwater prospect with lower fracture pressure due to large portions of water in the overburdens, leaving only a narrow pressure window for drilling operation. Due to the limitations of the narrow pressure window, there is a need for precise-control of the bottomhole pressure to keep it within this tight window.

$$BHP = MW + \Delta AFP \tag{2.1}$$

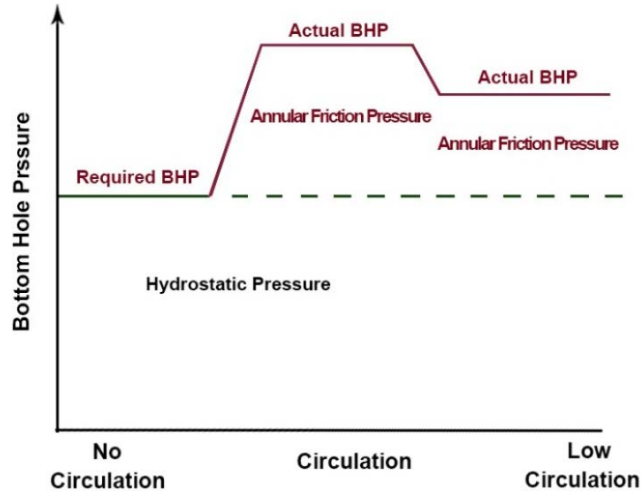


**Figure 2.3: Pressure Profile in Conventional Drilling Operation.**  
**Redrawn from Weatherford**

MPD provides a more accurate control of downhole pressure because of the pressurized closed-loop system, in which a rotating control device seals the top of the annulus and the flow of the well is controlled by a choke manifold to apply a backpressure. This is typically achieved by using drilling fluid with the same or slightly lower density than the pore pressure, and as a result of annular friction loss due to mud circulation, the ECD will be slightly higher than the pore pressure and stay below the fracture pressure (Hannegan, 2006). Meanwhile in the case low-/no-flow during connection, the loss of annular frictional pressure will be compensated by applying the backpressure from the choke adjustment at the surface. Therefore, the bottomhole pressure will always stay above the pore pressure and below the fracture pressure either during normal mud circulation or during connection with no circulation. This is the main reason the MPD helps to avoid many drilling-related issues, especially in narrow pressure window environment. In addition, MPD system allows a faster corrective action to deal with observed pressure variation compared to mud weight and pump rate adjustments alone and in general it provides a precise control for the bottomhole pressure to be within its pressure window.

$$BHP = MW + \Delta AFP + \Delta BP \quad (2.2)$$

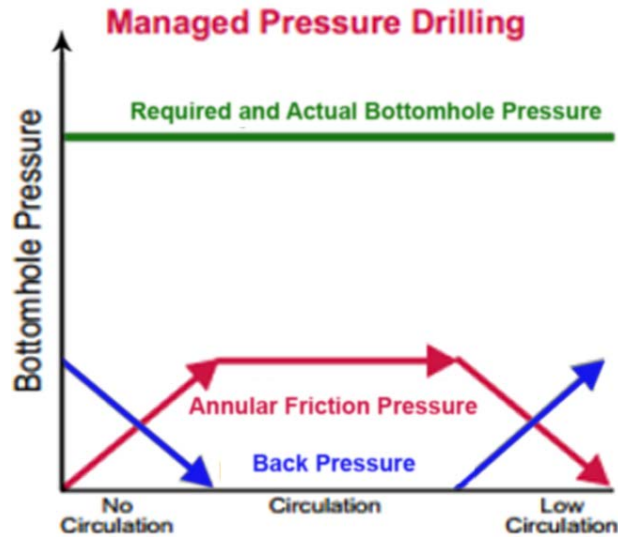


**Figure 2.4: Pressure Profile in Managed Pressure Drilling Operation.**  
**Redrawn from Weatherford**

### 2.1.3 Benefits of MPD

One of the main benefits of MPD is that it allows drilling operation into formations with narrow operating window between pore pressure and fracture pressure. The operational window during conventional drilling is illustrated in Figure 2.5. In the case of pressure window is sufficiently wide, stopping the circulation during connection might keep the ECD within the pressure window limit, therefore conventional drilling is acceptable in this case.

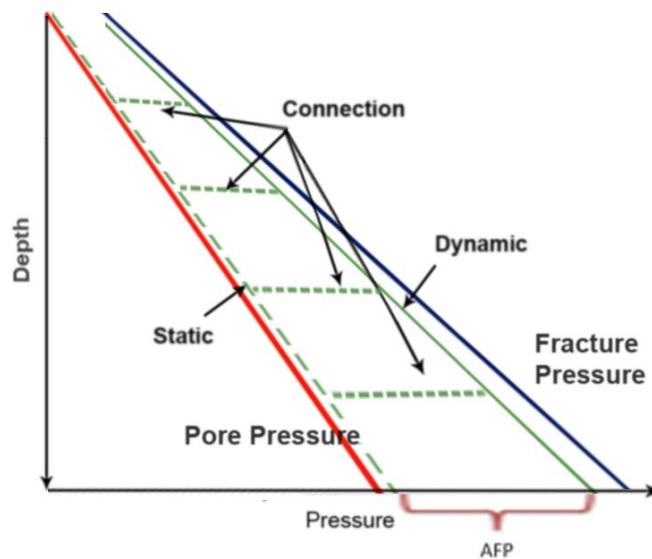


**Figure 2.5: Normal Operational Window. Redrawn from Thompson (2012)**

However, Figure 2.6 shows the case where the operational window is quite narrow. In this case, if conventional drilling methods are employed, then downhole pressure during connections will no longer be within the safe operational window as shown in the following figure. In this case, the bottomhole pressure falls below pore pressure, indicating that during connections we will encounter a kick if we are drilling into a permeable zone. This case demonstrates one of the main application areas for managed pressure drilling.

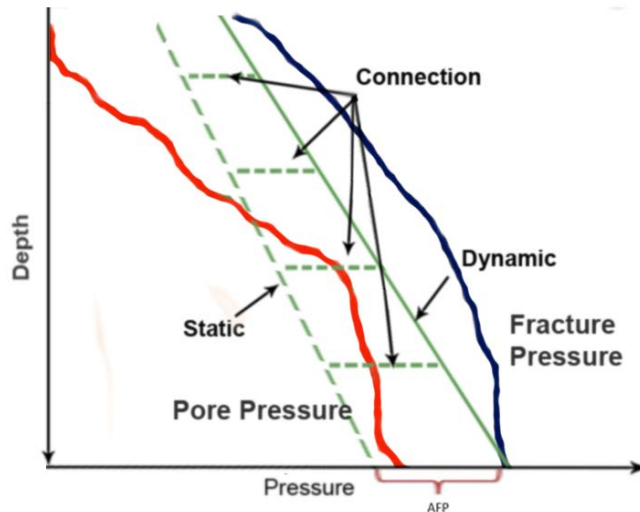


**Figure 2.6: Narrow Operational Window. Redrawn from Thompson (2012)**

In general, the ability of MPD system to maintain the downhole pressure within the narrow pressure window offer a wide range of benefits (Hannegan, 2006; Rehm et al, 2008), such as:

- Avoid drilling hazards such as kick, lost circulation, differential sticking, and wellbore stability, thereby reducing the non-productive time (NPT)
- Enhance the efficiency of drilling operation by improving the rate of penetration (ROP) and prolongs bit life
- Reduce the number of casing string, deepening casing set points and avoid failure to reach TD with large enough hole diameter
- Minimizes health, safety and environmental (HSE) risks
- Enables the drilling of otherwise un-drillable wells

With all the benefits of using MPD technology, the remaining prospects in the more challenging environment such as offshore, deepwater, HPHT well, areas with total loss formation that considered

as un-drillable with conventional drilling methods will become available. Thereby without this technology, much of the world resources will be neglected.

In order to have complete picture of MPD technology, the following list shows challenge and limitation for the technology to be implemented

- Costly operation
- More complicated operation
- Specially trained personnel are required to work on MPD operations
- It has slightly different approach compared to the conventional drilling operation, therefore well-established industry standards and work procedures are required for safe and efficient MPD operations

#### **2.1.4 MPD Techniques and Tools**

There are many variations of MPD techniques and some of the common MPD techniques include constant bottomhole pressure (CBHP), pressurized mud-cap drilling (PMCD), dual-gradient drilling (DGD) and also riserless drilling (Rehm et al, 2008; Nauduri et al, 2009). Each of the following techniques is addressed for drilling hazards to which it has proved applicable:

- **Constant Bottom Hole Pressure (CBHP):** A technique to maintain the precise balance between the pore pressure and fracture pressure. The bottomhole pressure variation in narrow pressure window, such as when pumping stops during drilling connection, are often the root causes for drilling-related issue such as kick, lost circulation, wellbore stability etc. By using rotating control device and choke manifold, it allows a faster corrective action to maintain the bottomhole pressure within its safe pressure window compared to mud weight and pump rate adjustments alone. This technique is often used to compensate the loss of frictional pressure while the mud circulation stopped by applying the backpressure from the choke manifold at the topside.

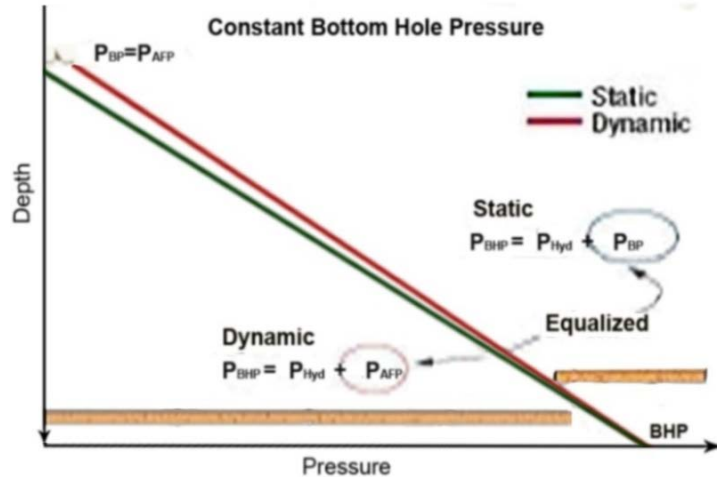


**Figure 2.7 Pressure Profile in Constant Bottomhole Pressure. Redrawn from Malloy (2007)**

- Pressurized Mud Cap Drilling (PMCD): A technique to safely drill into total loss formation or formations with large voids such as caverns. A heavy, viscous mud is pumped down the annulus and the annular fluid column will act as a cap or annular barrier, while a sacrificial drilling fluid, such as seawater, is used to drill into the total loss formation. The mud cap is maintained above the total loss formation that is taking the sacrificial drilling fluid and cuttings, therefore helping to stabilize the formation, preventing dangerous gasses flowing to the surface and minimize associated NPT while drilling into a total loss formation.

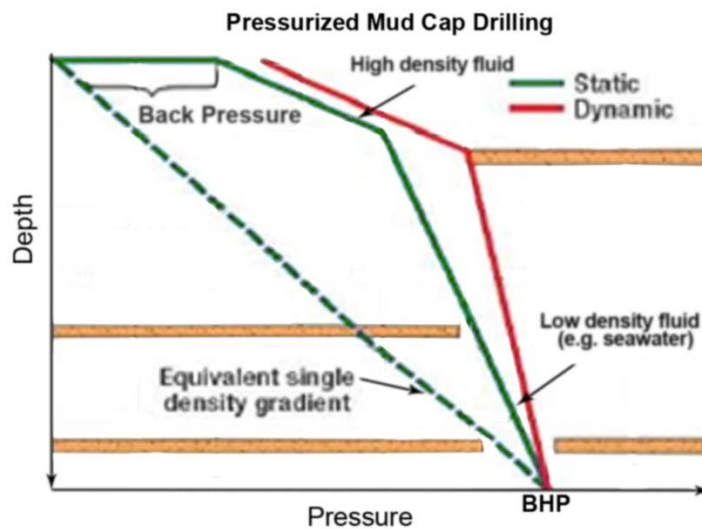


**Figure 2.8: Pressure Profile in Pressurized Mud Cap Drilling. Redrawn from Malloy (2007)**

- Dual Gradient Drilling (DGD): In DGD, the wellbore is drilled with two different annulus fluid gradients in place either by injecting lightweight fluid into the annulus with a parasite string or by having a mud-lift pump to circulate out the drilling fluid with the cutting through a return line instead of the marine riser. By having two distinct pressure gradients, a favorable pressure profile in deepwater wells is expected specifically a profile closer to what naturally exists in the formations. This is because the deepwater formation will have lower overburden pressure and fracture pressure due to the pressure gradient from seawater instead of the pressure exerted by the typical sand-shale formation. As a result, the utilization of dual gradient drilling will reduce the number of casing strings required, reduce the non-productive time and also enhance well control, therefore it is possible for deepwater drilling resource to be drilled and developed safely and economically.

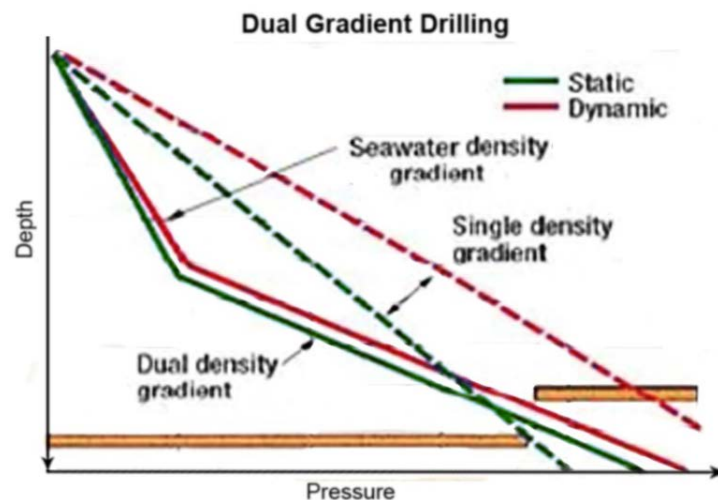


**Figure 2.9: Pressure Profile in Dual Gradient Drilling. Redrawn from Malloy (2007)**

- Riserless Drilling: A type of MPD technique which involves mud circulation during drilling without the use of a riser. When it comes to deepwater and HPHT applications, risers are considerably long with increased wall thickness. As a result, riser systems become quite expensive and also reduces options when it comes to choosing rigs as specialized rigs are needed to be able to handle heavy risers. In such a scenario, riserless drilling may be employed. In this technique, a separate mud return line is used to transport the returns from seabed to rigfloor. A subsea pump connected to a Rotating BOP (RBOP) diverts the returns to this mud return line. A schematic of riserless drilling is shown below in Figure 2.10. Such a riserless



drilling method has been developed by the company AGR and commonly referred to as RMR™ or Riserless Mud Recovery.

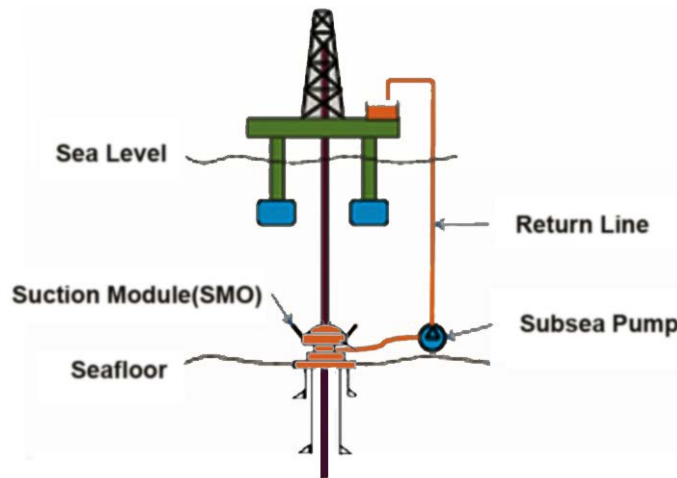


**Figure 2.10: Schematic of Riserless Drilling. Redrawn from [www.drillingcontractor.org](http://www.drillingcontractor.org)**

Managed-Pressure Drilling (MPD) employs both pressurized closed-loop drilling system and specialized equipment that allows potentially greater and more precise control of the downhole pressure profiles. Most of MPD variations requires at least a rotating control device (RCD), an MPD choke manifold and at least one non-return valve (e.g., floats) (Rehm et al, 2008; Nas et al, 2009). These tools are briefly explained below.

- **Rotating Control Device (RCD):** It is the main equipment in Managed Pressure Drilling. RCD is designed to seal off the wellbore and divert the flow from the annulus to the choke manifold through a flow spool beneath the RCD. It has an advanced compound sealing rubber and a sealing sleeve that allows rotation and vertical movement of drill pipe, while providing a required seal for the annulus. In addition, it has a rubber element on the bearing in order to reduce wear (Chrzanowski, 2011).

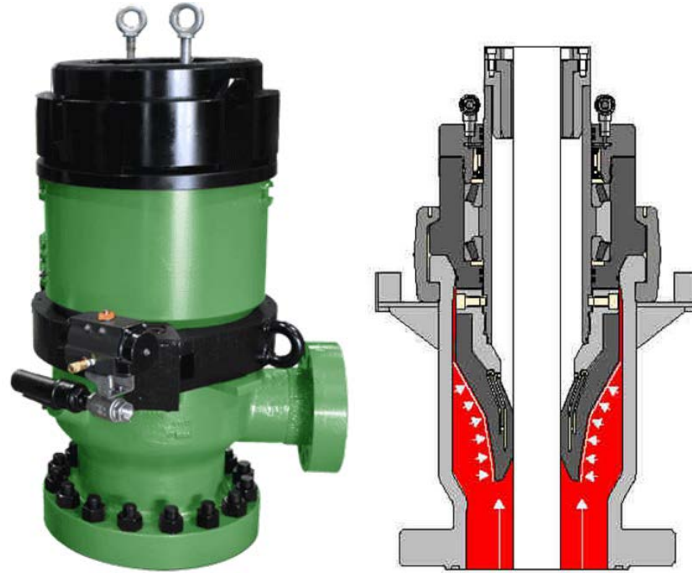


**Figure 2.11: Rotating Control Device (Smith Services)**

- **Drilling Choke Manifold:** It is used to control the annular backpressure by adjusting the opening of the choke. The chokes are installed in the return flow line to allow back pressure to be applied during the drilling process and there should be two chokes mounted in parallel in case one of them gets plugged. The mud returns are circulated through the choke and when the choke is fully open there will only be little or no backpressure. Meanwhile in the case of no flow such as during connection, the choke need to be closed quickly to trap the pressure. A dedicated backpressure pump should be available in the case of no flow in order to boost the necessary backpressure. The choke system can be controlled manually, semi-automatic or fully automatic. In the fully automatic system, the chokes are hydraulically controlled by a Programmable Logic Controller (PLC) system. PLC adjust the choke opening based on real-time data measurement and the pressure and flow dynamics from the hydraulic model. The choke system in Managed Pressure Drilling is part of the continuous MPD operation to control the bottom hole pressure and should not be considered as secondary well control equipment as in the case of conventional drilling choke.

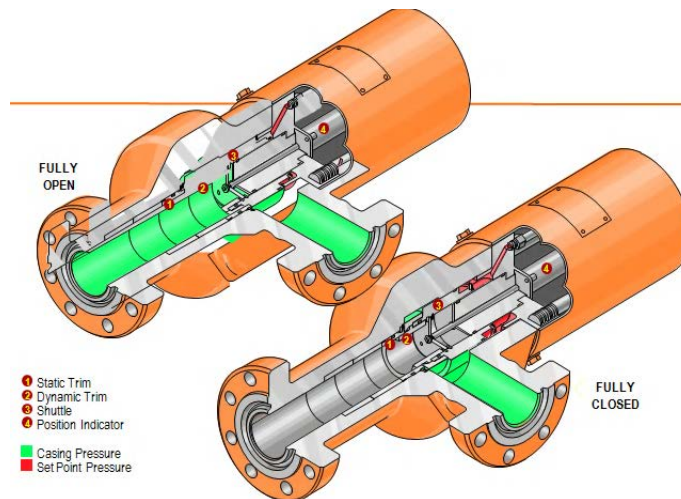


**Figure 2.12: Operation Principle of Semi Auto Choke (Arnone, 2010)**

- Non-Return Valve (NRV): It only allows a downward flow of mud inside the drillstring. NRV or known as float valve are installed in the BHA to prevent the u-tube situation due to the positive unbalance in the annulus that forces drilling fluid to flow back up to the drillstring. In the case of MPD operation, the applied backpressure in the annulus might force the drilling fluid to flow back up to the drillstring, carrying cutting that can plug the bit, MWD and motor assembly. NRV is essential in MPD operation, because in order to control the bottomhole pressure some amount of back pressure is applied to compensate the annular friction losses. The NRV will keep the positive backpressure because of the restriction of flow up to the drillstring. Two types of NRV that are commonly used are the flapper floats and plunger floats.



**Figure 2.13: Non-Return Valves ([www.drillingformula.com](http://www.drillingformula.com))**

- Coriolis flowmeter: Coriolis flowmeter is used to provide an accurate measurement of mass flow, volumetric flow rates, and density. The main benefits of using Coriolis flowmeter in MPD operation is to accurately identify kick because it is not possible to perform conventional flow check in the closed-loop MPD system.



**Figure 2.14: Coriolis Flowmeter ([www.drillingcontractor.org](http://www.drillingcontractor.org))**

- Surface separation equipment: MPD techniques are intended to keep out gas influx during drilling. However, the MPD system typically has a surface separation equipment to handle unwanted influx and to monitor returns.



**Figure 2.15: MPD Multiphase Separation System (Sveinall, 2010)**

## **2.2 PRESSURE ESTIMATION IN MANAGED PRESSURE DRILLING**

In most MPD operation, the downhole pressure is used as the variable to control. There are two ways to estimate and control the downhole pressure, the indirect and the direct control. The indirect control uses measurements from choke manifold at the topside and then the downhole pressure is estimated by using either simulation or observer. Then, the mathematical model needs to be designed for the simulation or observer to estimate the downhole pressure. Meanwhile, the direct control uses measurements directly from the downhole using PWD tools or mud-pulse telemetry. Estimation and control of the downhole pressure based on the downhole measurement might not be reliable because these sensors are very expensive and the data obtained are often noisy, and also due to slow sampling, transmission delays, loss of communication for low or no-flow conditions (Hasan, 2014). Consequently, the topside measurement will act as a control input for downhole pressure estimation. Therefore, a pressure estimation scheme is required to accurately estimate the downhole pressure from the measurement at the surface (Stamnes, 2011).

The downhole pressure profile can be difficult to obtain as it is a complex function of drilling parameter such as friction, density, etc. A simplified hydraulic model that capture the dominant phenomena of the drilling system has been considered as the more convenient solution than the advanced hydraulic model, because in most cases the available data contain insufficient information

for an advanced hydraulic model. In addition, several drilling parameters such as friction coefficient throughout the wellbore and the influx or out flux (loss circulation) rate are both uncertain as there is no direct way to measure them and also slowly changing. This simplified hydraulic model that is derived from mass balance equation and a simplified momentum balance can describe the flow and pressure dynamics along the wellbore (Kaasa et al, 2011). Using a PDE model of simplified hydraulic that captures the dominant phenomena of the drilling system, the physical system of MPD can be modeled in  $2 \times 2$  linear hyperbolic system. The specific class of this hyperbolic system has been studied in recent years for many fluid flow systems such as flow in transmission lines (Curro, Fusco, and Mangarano, 2011), gas flow pipelines (Gugat and Dick, 2011), mud flow in annulus of the wellbore (Kaasa, 2012; Hauge, 2013). In order to have an estimation scheme for wellbore hydraulics in MPD operation, the infinite dimensional system of PDEs are discretized as a finite high-dimensional approximation in ODEs or known as early lumping approach. As a result, the linear hyperbolic system can be written into a lumped model. Therefore, the flow and pressure dynamics of the MPD system can be expressed as a state space representation that can be solved by numerical simulation.

### **2.2.1 Adaptive Observer**

An adaptive observer is used to estimate unmeasured states in a dynamic system with parametric uncertainties. In an MPD operation, the pressure profile throughout the wellbore is not measured and the data quality for feedback control is low due to the noise, slow sampling rates and loss of communication. Due to the lack of measurement for the control purposes, an estimation scheme for pressure and flow dynamics of the wellbore is important for control design in MPD system. In addition to estimating the pressure and flow dynamics, an adaptive observer can also be used to estimate parameter uncertainties such as friction, influx, and fluid loss (Stamnes, 2011). Based on the available measurement at the topside, these unmeasured data can be estimated by adjusting the dynamic system of wellbore hydraulics.

Kalman (1960) presented an estimation of the dynamic system using stochastic approach or well-known as filter or an estimator. Meanwhile, an observer is a term for the estimation of the dynamic system using deterministic approach. An observer is mainly used to estimate the dynamic system while the parameters are well-known. On the other hand, an adaptive observer is useful in the case

of uncertain parameters in the system. As in the case of MPD, there are uncertain parameters such as friction, influx and fluid loss that need to be accurately estimated in order to have an accurate estimation of the state system, that is pressure dynamics of the wellbore.

An adaptive observer design for  $2 \times 2$  linear hyperbolic system needs to be carefully reviewed for the application of wellbore hydraulic system in Managed Pressure Drilling. There have been some literature that propose methods for control design in this specific class of PDEs, including using control Lyapunov functions (Coron, d'Andrea Novel, and Bastin; 2007), Riemann invariants (Greenberg and Tsien;1984) and frequency domain approaches (Litrico and Fromion; 2006).

The recent method for control of PDEs is called Backstepping method (Krstić and Smyshlyaev; 2008). The backstepping method was actually a well-known method in nonlinear control theory for finite dimensions problem (Khalil; 2002, and Kokotović; 1992), where it starts by establishing a controller that stabilized the inner sub-systems before gradually "backs out", and then setting up new controllers that in turn stabilize the outer subsystems before the overall system is stabilized. Bosković, Krstić, and Liu (2001) also developed a backstepping-like transformation in order to stabilize an unstable heat equation. This method had few similarities with the earlier finite-dimensional problem, with the nested subsystems emerging from the discretization of the PDE into a finite number of control volumes. For the stabilization of the remaining control volumes, a controller was designed for the innermost control volume, before gradually "backing out" and then simultaneously extending the stabilization of the controller. Bosković et al. (2001) and Balogh and Krstić (2002) proposed a method that restricts the system with a number of open-loop unstable eigenvalues. This method involved recursively solving a series of equations for the unknown controller gains - frequently referred to as kernels used in the backstepping. As a result, an arbitrary level of instability was allowed by using the backstepping method on a semi-discretized version of the system making the close loop system stable (Anfinsen, 2013).

The solutions of the kernel equations are required in order to implement the observer on a numerical simulation. Vazquez and Krstić (2013) proposed an explicit equation to the subsystem for the kernel equations by assuming that it has constant coefficients. The solution uses Bessel functions and generalized Marcum Q-functions of the first order. According to Vazquez (2013), there were two methods for solving the kernel equations. One of the alternatives is to discretize the PDEs. By discretizing the PDEs, there will be discontinuities to the system, and the number of discontinuities

tends towards infinity. Smyshlyaev and Krstić (2004) proposed an alternative by using a discretization method averaging certain terms, instead of using their exact values. However, the solution was only applicable for certain boundary conditions. In order to apply the solution for another boundary conditions of kernel equations, one can use a method of characteristic that was presented in Vazquez (2013). This method can be used to proof the existence and uniqueness for specific kernels equations (Anfinsen, 2013).



### **3. HYDRAULIC WELL MODEL**

Automation in Managed Pressure Drilling operation relates to the control system that regulates the choke opening at the topside facility in order to maintain the downhole pressure. The automated MPD system requires a hydraulic well model that estimates the downhole pressure and a feedback control that automatically regulate the choke opening to maintain the required choke pressure according to the set point. Hence, the hydraulic well model plays an important role in determining the accuracy of the MPD system.

For the selection of a mathematical model that represent the MPD system, there are at least two important factors that need to be considered. First, the model should consider as many variables in wellbore hydraulics such as friction and gravity, without being so complex as to require expert knowledge to setup and adjust, and the second is that the model should be able to be automatically calibrated with existing measurement (Kaasa et al, 2011). The main challenge here is to remove unnecessary dynamics such that the model includes only the dominating dynamics of the system while still achieving satisfactory accuracy. A fit-for-purpose modeling is important to understand the importance of the various dynamics in the system in order to figure out the suitable trade-off between accuracy and simplicity.

This chapter presents a simplified hydraulic model based on basic fluid dynamics that captures the dominant phenomena of the MPD system. In the following section, the approach for fit-for-purpose modeling, the main simplification and the derivation of the simplified hydraulic model is outlined. A thorough derivations of the simplified hydraulic model can be found in Kaasa (2007) and Kaasa et al. (2011). The model has also been used in Stamnes et al. (2008), Zhou et al. (2011), Godhavn et al. (2011), Hauge (2013), and Hasan (2014) in order to estimate the downhole pressure, kick scenario, and pressure control etc.

#### **3.1 FIT FOR PURPOSE MODELLING**

It is important to understand the objective of the modeling before establishing the mathematical model of wellbore hydraulics that will be used in this work. The main objective of the hydraulic model is to estimate the pressure and flow dynamics of the wellbore and to estimate the unknown

parameter along the wellbore in order to determine the required backpressure from the choke based on the estimation of the downhole pressure (Stamnes, 2011). In addition, the relationship between the choke system and the downhole pressure should be reflected by the hydraulic model in order to allow the feedback control to provide a set point for the choke system based on the estimation of the downhole pressure.

In order to estimate the dynamics of drilling hydraulics, there has been some work to develop both advanced hydraulic well model and simpler, more transparent model. The advanced models capture some particular aspects of drilling hydraulics that is useful for detailed simulation of some specific events or problems during a drilling operation and to improve the accuracy of the MPD system. However, in most cases, the available data contain insufficient information for an advanced hydraulic model. As a result, parameter estimation scheme might not be able to provide the result even for some of the main parameters. Due to the uncertainties, unknown parameters and also a lack of additional distributed measurement along the well during an MPD operation, most of the detail of advanced hydraulic model does not contribute to improving the accuracy of the downhole pressure. For the design of the control system, the use of advanced hydraulic model leads to higher level of complexity and higher frequency dynamics, so that the control system might not be able to compensate for changes that are faster than the dynamic response of choke valve and sampling rate. The control system is ineffective to response to the dynamics that are much faster than the bandwidth of the closed-loop system (Kaasa et al, 2011).

Another issue with the use of a complex hydraulic model is related to the verification of numerical simulation of a control system based on the advanced model. Several parameters during drilling operation such as friction coefficient throughout the wellbore, the influx or outflux (loss circulation) rate, the amount of gas dissolved in the drilling fluid are both uncertain and slowly changing. An online parameter estimation is important to allow model calibration in order to improve the accuracy. However, the use of a complex model makes it difficult to create parameter estimation scheme that allows model calibration due to the presence of countless and complex parameter.

With the main task of this work being system identification and the main objective is to estimate the system states and the unknown parameters for the hydraulics of MPD, then a simpler, more transparent hydraulic model will be the more convenient alternative compared to the advanced

hydraulic well model. It is important for the simplified hydraulic model to capture most dominant dynamics in order to have a suitable representation of wellbore hydraulics and to accomplish good accuracy of the system. In the following section, the fit-for-purpose model is obtained by neglecting the high-frequency dynamics that the control system is not able to compensate, neglecting the slow dynamics that can be handled more efficiently by feedback from measurement and lump together that are not possible to distinguish from one another in the available measurements.

### 3.2 OUTLINE OF MODEL DERIVATION

The wellbore hydraulic model is derived based on the assumption that the drilling fluid can be treated as a viscous fluid. It means that the flow can be described by the following fundamental equations (Merritt, 1967 and White, 1994).

- Fluid viscosity: the viscosity as a function of pressure and temperature.
- Equation of state: the density as a function of pressure and temperature.
- Conservation of mass: the mass balance or equation of continuity.
- Conservation of momentum: the force balance or Newton's second law of motion.
- Conservation of energy: the energy balance or the first law of thermodynamics.

The formulation of continuity, momentum, and energy equation that will be used as the foundation of hydraulic model are based on the following assumptions:

- Flow can be treated as 1D along the main flow path
- Flow is radially homogeneous
- Incompressible flow, so that the spatial time variance is negligible in the momentum equation
- Time variance of the viscosity is negligible in the momentum equation

In addition, the effect of the temperature with the dynamics in the energy equation will not be considered in the following model.

### 3.2.1 Equation of State

An equation of state is a thermodynamic equation describing the constitutive mathematical relationship of a material or substance under a given set of physical conditions. In general, the equation of state is written as

$$\rho = \rho(p, T) \quad (3.1)$$

The equation of state cannot be derived from physical fundamental principles. Instead, it can be found empirically from PVT data using interpolation of pressure and temperature dependency. The changes in density are generally small for a liquid, which makes it common to use the linearized equation of state around the reference point.

$$\rho = \rho_0 + \frac{\partial \rho}{\partial p}(p - p_0) - \frac{\partial \rho}{\partial T}(T - T_0) \quad (3.2)$$

where  $\rho_0, p_0, T_0$  is the reference point for the linearization. Combining the isobaric cubical expansion coefficient ( $\alpha$ ) and the isothermal bulk modulus ( $\beta$ ) that is reciprocal of the compressibility of the fluid,  $c = 1/\beta$ , and a property that determine the dominating pressure transient in the system which is defined as

$$\beta = \rho_0 \left( \frac{\partial p}{\partial \rho} \right)_T \quad (3.3)$$

$$\alpha = -\frac{1}{\rho_0} \left( \frac{\partial \rho}{\partial T} \right)_p \quad (3.4)$$

then the linearized equation of state can be written as follows

$$\rho = \rho_0 + \frac{\rho_0}{\beta}(p - p_0) - \rho_0 \alpha (T - T_0) \quad (3.5)$$

or

$$\partial \rho = \frac{\rho}{\beta} \partial p - \rho \alpha \partial T \quad (3.6)$$

The accuracy of linearization depends on the increase of pressure and temperature. However, for most drilling fluids in the ranges of 0 – 500 bar and 0 - 200°C, the linearization shows a fairly accurate result.

Compared to the pressure transients, which are in the range of seconds to minutes, the temperature transients are much slower in the range of minutes and hours. The thermal expansion coefficient ( $\alpha$ ), which represent the temperature changes with respect to transient effects, are usually small for liquids. As a result, transient temperature effect is slower compared to the pressure transient effect, so that the slow pressure effect due to the temperature changes can be handled by online calibration based on feedback from measurements. The simplified dynamic model for pressure transients in the system that neglect the dependence on the temperature can be written as

$$\partial\rho = \frac{\rho}{\beta} \partial p \quad (3.7)$$

### 3.2.2 Equation of Continuity

Assuming that the flow is radially homogeneous and one-dimensional flow along the flow path, the differential continuity equation is given by

$$\frac{\partial\rho}{\partial t} + \frac{\partial}{\partial x}(\rho v) = 0 \quad (3.8)$$

where  $v$  is the velocity of the flow, and  $x$  is the spatial variable along the flow path. By substituting Eq. (3.7) into Eq. (3.8), the expression of pressure dynamics can be written as

$$\frac{\partial p}{\partial t} = \frac{\beta}{\rho} \frac{\partial\rho}{\partial t} = -\frac{\beta}{\rho} \frac{\partial}{\partial x}(\rho v) = -\frac{\beta}{\rho} \left( \frac{\partial\rho}{\partial x} v + \frac{\partial v}{\partial x} \rho \right) \quad (3.9)$$

Assuming that the flow is incompressible and that the cross-sectional area  $A(x)$  is constant, then the expression of pressure dynamics can be rewritten with explicit dependence on time and spatial position as follows

$$\frac{\partial p}{\partial t} = -\beta \frac{\partial v}{\partial x} = -\beta \frac{\partial \left( \frac{q}{A(x)} \right)}{\partial x} = -\frac{\beta}{A} \frac{\partial q}{\partial x} \quad (3.10)$$

The assumption of incompressible flow means that the effects of density to the flow characteristic are neglected. The main compressibility effects are taken into account through the variable bulk modulus ( $\beta$ ) from the equation of state that characterizes the dominating dynamics of the hydraulic system and reflected in the pressure along the flow path. As a result, the pressure dynamics at any point in the well can be approximated by the dynamics of average pressure in the entire well. By using integration of mass flow over a control volume ( $V$ ), then the mass balance can be written as

$$\frac{d}{dt}(\rho V) = \rho_{in} q_{in} - \rho_{out} q_{out} \quad (3.11)$$

where  $\rho$  is the average density,  $w_{in} = \rho_{in} q_{in}$  and  $w_{out} = \rho_{out} q_{out}$  are the mass flow rate. In order to have pressure as the main variable, the density dynamics from Eq. (3.7) need to be substituted as

$$\rho \frac{V}{\beta} \frac{\partial p}{\partial t} = -\rho \frac{dV}{dt} + \rho_{in} q_{in} - \rho_{out} q_{out} \quad (3.12)$$

By assuming a homogeneous density along the well,  $\rho_{in} = \rho_{out} = \rho$ , then the expression for pressure dynamics can be simplified as follows

$$\dot{p} = -\frac{\beta}{V} (q_{out} - q_{in} + \dot{V}) \quad (3.13)$$

### 3.2.3 Equation of Momentum

White (1994) develop a force balance based on conservation of momentum for one-dimensional time invariant density and viscosity. It is assumed that the flow can be treated as one-dimensional flow along the path. As a result, the differential equation is simpler than the three-dimensional flow but still relatively accurate. The resulting partial differential equation can be written as

$$\rho \frac{dv}{dt} = -\frac{\partial p}{\partial x} - \frac{\partial \tau}{\partial x} + \rho g \cos \theta \quad (3.14)$$

where  $\rho$  is the mud density,  $v$  is the velocity of the flow,  $x$  is the spatial coordinate along the path,  $\tau$  is the viscous frictional force per spatial unit,  $g$  is the gravitational constant, and  $\theta$  is the slope of the flow path at  $x$ . By assuming that the cross-sectional area  $A(x)$  is constant, then Eq. (3.14) can be rewritten with flow rate  $q$  as the main variable

$$\frac{\rho}{A} \frac{dq}{dt} = -\frac{\partial p}{\partial x} - \frac{\partial \tau}{\partial x} + \rho g \cos \theta \quad (3.15)$$

The friction term  $\tau$  is a lumped friction term that is depending on the velocity of flow. It represents the term minor losses that account all frictional loss such as viscous dissipation, turbulence, swirl flow, and non-ideal flow conditions due to restrictions, section changes, bends, etc.

The speed of sound characteristic can be found from the Newton-Laplace equation that shows the relationship between density and compressibility. It relates to the pressure transients that propagate as pressure waves in the fluid. The speed of sound is given by

$$a = \sqrt{\frac{\beta}{\rho}} \quad (3.16)$$

The dynamics of the propagation of pressure transients are typically very fast for a hydraulic oil, and often it is much faster than the bandwidth of the MPD control system. As a result, it is reasonable to neglect this variable in the hydraulic model.

The flow dynamics Eq. (3.15) that is expressed in partial differential equation can be approximated by assuming that the fluid accelerates homogeneously as a stiff mass. The simple equation for the average flow rate dynamics can be obtained by integration of Eq. (3.15) based on

$$M(l_1, l_2) \frac{dq}{dt} = p_1 - p_2 - F(l_1, l_2, q, \mu) + G(l_1, l_2, \rho) \quad (3.17)$$

where

$$M(l_1, l_2) = \int_{l_1}^{l_2} \frac{\rho(x)}{A(x)} dx \quad (3.18)$$

$$F(l_1, l_2, q, \mu) = \int_{l_1}^{l_2} \frac{\partial \tau(\frac{q}{A(x)}, \mu)}{\partial x} dx \quad (3.19)$$

$$G(l_1, l_2, \rho) = \int_{l_1}^{l_2} \rho(x) g \cos \theta(x) dx \quad (3.20)$$

where  $M(l_1, l_2)$  is the density per cross-section integrated over the flow path,  $F(l_1, l_2, q, \mu)$  is the friction losses integrated along the flow path, and  $G(l_1, l_2, \rho)$  is the total gravity.

### 3.3 SIMPLIFIED HYDRAULIC MODEL

#### 3.3.1 Simplified ODE Model

Kaasa (2007) developed a third order model consists of nonlinear ODE's for MPD system that captures the dominant phenomena in the system. This model does not consider the fast dynamics in the system, and similar effects are lumped together while slowly varying parameters are treated as constants. The system as illustrated in Figure 3.1 is divided into two control volumes, the drill string and the annulus, because it is assumed that the flow pattern is uniform along each control volumes. As a result, the well can be considered as two separate control volumes with different dynamics (Kaasa, 2007). The drillstring part consist of topside assembly, drill pipes, the bottomhole assembly including MWD tool and the drill bit. Meanwhile, the annulus part consists of an open hole section, a cased hole section, and the choke manifold at the surface.

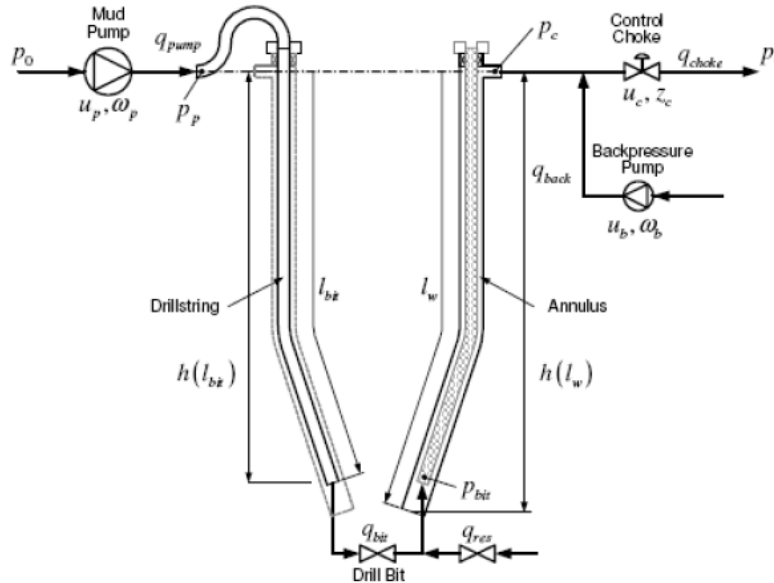


Figure 3.1: Simplified Schematic of the Drillstring and Annulus (Kaasa, 2007)



Using conservation of mass and momentum balances, the model is summarized in three ODEs equations, the main pump pressure equation and the choke pressure equation for the pressure dynamics and also the volumetric flow rates through the bit for the flow dynamics.

The pressure dynamics are derived based on mass balance, Eq. (3.13). The equation for the pump pressure is given by

$$\frac{V_d}{\beta_d} \dot{p}_p = q_{pump} - q_{bit} \quad (3.21)$$

where  $V_d$  is the volume of the drill string,  $\beta_d$  is the effective bulk modulus of the drill string,  $p_p$  is the pressure of the main pump,  $q_{pump}$  is the volumetric flow rates from the main pump,  $q_{bit}$  is the volumetric flow rates through the bit.

The equation for the choke pressure can be written as follows

$$\frac{V_a}{\beta_a} \dot{p}_c = q_{bit} + q_{back} - q_{choke} + q_{res} - \dot{V}_a \quad (3.22)$$

where  $V_a$  is the volume of the annulus,  $\beta_a$  is the effective bulk modulus of the annulus,  $\dot{V}_a$  is the change in volume in the annulus,  $p_c$  is the pressure of the choke,  $q_{res}$  is the reservoir influx,  $q_{back}$  is the backpressure pump flow, and  $q_{choke}$  is the volumetric flow rates through the choke.

The flow dynamics is derived from a momentum balance, Eq. (3.17) and it is governed by:

$$M \dot{q}_{bit} = p_p - p_c - F_d |q_{bit}| q_{bit} - F_a |q_{bit} + q_{res}| (q_{bit} + q_{res}) + (\bar{\rho}_d - \bar{\rho}_a) g h_{bit} \quad (3.23)$$

where  $M_a$  is the mass coefficient of the annulus,  $M_d$  is the mass coefficient of the annulus,  $F_d$  is the frictional pressure drop coefficients in the drillstring,  $F_a$  is the frictional pressure drop coefficients in the annulus,  $h_{bit}$  is the true vertical depth (TVD) of the bit,  $\bar{\rho}_d$  is the average density in the drill string,  $\bar{\rho}_a$  is the average density in the annulus, and  $g$  is the acceleration of gravity. The mass coefficient (integrated density per cross section)  $M$  is given by  $M = M_a + M_d$ , where  $M_j = \int_0^{L_j} \rho_j(x) / A_j(x) dx$ .

The equation for the pressure at the bit or known as bottomhole pressure will be the sum of hydrostatic pressure, frictional pressure along the annulus, choke pressure and pressure due to the rate of change in  $q_{bit}$  as given by

$$p_{bit} = p_c + M_a \dot{q}_{bit} - F_a |q_{bit} + q_{res}|(q_{bit} + q_{res}) + \rho_a g h_{bit} \quad (3.24)$$

Using this model, the control system in MPD operation will be designed to control the  $q_{choke}$  by using some inner control loop to set the choke opening,  $z_c$ , in order to maintain the bottom hole pressure. The equation for the flow through the choke based on the orifice equation (Merritt, 1967) is given by

$$q_{choke} = K_c z_c \sqrt{\frac{2}{\rho_a} (p_c - p_o)} \quad (3.25)$$

where  $K_c$  is the choke valve constant related to the valve characteristic,  $z_c \in [0,1]$  is the choke opening, and  $p_o$  is the atmospheric pressure.

### 3.3.2 Simplified PDE Model

In order to have a hydraulic well model that will provide better estimation on the downhole pressure and flow dynamics of a well, we will consider the model in sets of partial differential equation (PDEs) form. In order to implement this PDEs for the simulation, these equations will be discretized into a large set of ordinary differential equations (ODEs) that can be used to estimate the pressure and flow dynamics once all the data and parameters are fed into the simulators.

White (2007), Kaasa et al. (2012), and Landet et al. (2013) proposed a hydraulic well model for fluid flow through the annulus. Assuming drilling fluid as a viscous fluid in order to fulfill the fundamental relations such as equation of state, mass conservation, momentum conservation and energy conservation as explained in Section 3.2.1 – 3.2.3, then the mass conservation for the case of single phase and one-dimensional flow can be written as follow

$$\rho_t(z, t) = -\frac{1}{A_a} m_z(z, t) \quad (3.26)$$

where  $t \in [0, l]$  is the time instant,  $z \in [0, l]$  is the spatial coordinate along the annulus, from bottomhole  $z = 0$  up to the annulus and to the topside  $z = l$ ,  $\rho$  is the mud density,  $A_a$  is the cross section area of the annulus and  $m$  is the mass flow. Using the definition of bulk modulus  $\beta = \rho p_\rho$ , then we can write Eq. (3.26) as

$$p_t(z, t) = -\frac{\beta}{A_a} q_z(z, t), \quad (3.27)$$

where  $p$  is the annular pressure,  $\beta$  is the bulk modulus,  $q$  is the mud volumetric flow rate through the annulus. The momentum conservation derived from Eq. (3.17) – (3.20) can be written as

$$m_t(z, t) = -A_a p_z(z, t) - A_a \frac{\partial}{\partial z} \int \rho v^2 dA - Fq(z, t) - A_a g \sin \tau(z) \quad (3.28)$$

where  $v$  is the fluid velocity,  $F$  is the friction coefficient and  $g$  is the gravitational constant. Assuming the integral of  $\int \rho v^2 dA$  to be small enough and considering vertical well, the flow rate can be written as follow

$$q_t(z, t) = -\frac{A_a}{\rho} p_z(z, t) - \frac{F}{\rho} q(z, t) - A_a g, \quad (3.29)$$

The boundary conditions are given by

$$q(0, t) = q_b(t) = q_p(t) + q_i(t) \quad (3.30)$$

$$p(l, t) = p_c(t) \quad (3.31)$$

where  $q_b$  denotes the is mud flow rate at the bit,  $q_p$  denotes the mud flow rate from the main pump which is measured,  $q_i$  denotes volumetric in- or outflux which is an unknown parameter and  $p_c$  denotes the choke pressure which is the controlled input.

The frictional pressure loss in the annulus is given by

$$F = \varphi_1 q(z, t) + \varphi_2 q(z, t)^2 \quad (3.32)$$

where  $\varphi_1$  and  $\varphi_2$  denotes the frictional coefficients. For a laminar flow throughout the annulus (Reynolds Number,  $Re < 2000$ ), it will be modeled by setting  $\varphi_2 = 0$ . The frictional pressure

drop in the annulus is typically linear with respect to the flow. Therefore, the frictional pressure loss as a function of flow rate can be rewritten as

$$F = \varphi_1 q(z, t) \quad (3.33)$$

The term hydrostatic pressure due to gravity from the momentum equation can be removed by defining

$$\bar{p}(z, t) = p(z, t) - \rho g(l - z) \quad (3.34)$$

which gives

$$\bar{p}_t(z, t) = p_t(z, t) = -\frac{\beta}{A_a} q_z(z, t) \quad (3.35)$$

$$\begin{aligned} q_t(z, t) &= -\frac{A_a}{\rho} (\bar{p}_z(z, t) - \rho g(l - z)) - \frac{F}{\rho} q(z, t) - A_a g \\ &= -\frac{A_a}{\rho} \bar{p}_z(z, t) + A_a g - \frac{F}{\rho} q(z, t) - A_a g \\ &= -\frac{A_a}{\rho} \bar{p}_z(z, t) - \frac{F}{\rho} q(z, t) \end{aligned} \quad (3.36)$$

This gives

$$\bar{p}_t = -\frac{\beta}{A_a} q_z(z, t) \quad (3.37)$$

$$q_t = -\frac{A_a}{\rho} \bar{p}_z(z, t) - \frac{F}{\rho} q(z, t) \quad (3.38)$$

$$q(0, t) = q_p(t) + q_i(t) \quad (3.39)$$

$$p(l, t) = p_c(t) \quad (3.40)$$

## 4. TRANSFORMATION OF HYDRAULIC MODEL

As mentioned in the previous chapter, the hydraulics of MPD system can be described by a set of PDEs derived from mass balance and momentum balance equations. This PDE model for hydraulics in MPD system can be modeled using 2 x 2 linear hyperbolic partial differential equations (PDEs) (Hauge, 2013). This specific class of hyperbolic system has been studied in recent years for many fluid flow systems such as flow in transmission lines (Curro, Fusco, and Mangarano, 2011), gas flow pipelines (Gugat and Dick, 2011), mud flow in annulus of the wellbore (Kaasa, 2012; Hauge, 2013).

The infinite dimensional systems of PDEs need to be discretized as a finite dimensional approximation in ODEs in order to simulate the flow and pressure dynamics in the wellbore. By using a method of lines, the spatial coordinate ( $x$ ) can be discretized for N-nodes and as a result the 2 x 2 linear hyperbolic system can be written into a lumped model (Hasan and Imsland, 2014). Therefore, the flow and pressure dynamics of the hydraulic system can be expressed as a state space representation that can be solved by numerical solvers in the simulator.

### 4.1 MODEL TRANSFORMATION

A thorough transformation of the hydraulic model into a linear hyperbolic system can be found in Hauge (2013), and the discretization is explained in Hasan (2014). In order to develop the observer in 2 x 2 linear hyperbolic system, the hydraulic PDE model needs to be transformed into the following equation

$$u_t = -\epsilon_i(x)u_x + c_1(x)v, \quad (4.1)$$

$$v_t = \epsilon_2(x)v_x + c_2(x)u, \quad (4.2)$$

$$u(0, t) = qv(0, t) + v_i(t) + CX(t) \quad (4.3)$$

$$v(1, t) = U(t) \quad (4.4)$$

where the state  $u, v \in [0,1] \times [0, \infty)$ .  $\epsilon_1(x), \epsilon_2(x) > 0$ , the constant  $q \neq 0, v_i(t) \geq 0, c_1, c_2 \in [0,1]$ . The control input is  $U(t)$ , while  $u(x = 1, t)$  is the measurement at the topside facility. The subscripts  $x$  and  $t$  denote the partial derivatives with respect to spatial and time, respectively.

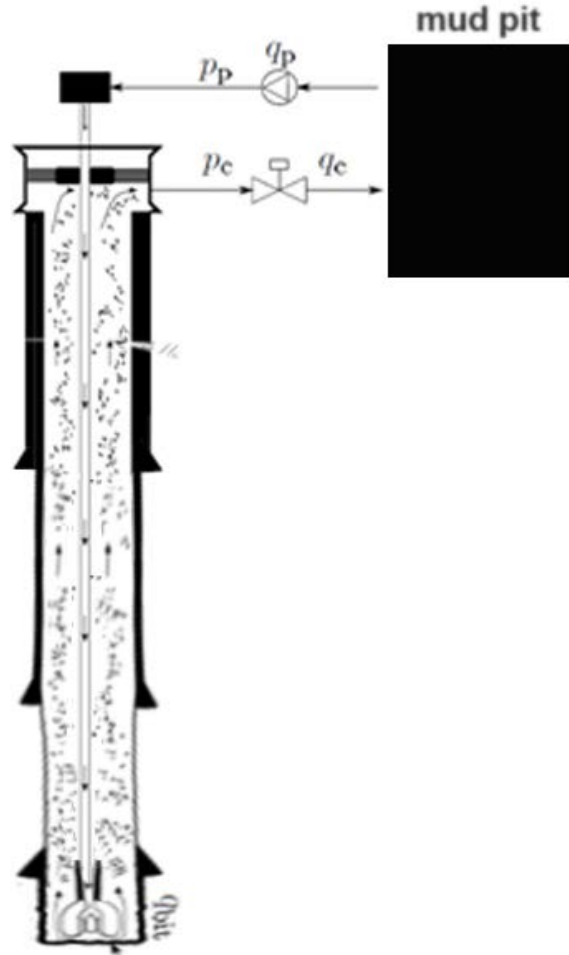


**Figure 4.1: Schematic of Managed Pressure Drilling System.  
Redrawn from Espen Hauge (2013)**

As mentioned in the previous chapter (Eq. 3.37 – 3.40), from the fundamental relations such as the mass conservation, and the simplified momentum conservation, the flow dynamics and pressure dynamics of wellbore can be written as

$$\bar{p}_t = -\frac{\beta}{A_a} q_z(z, t) \quad (4.5)$$

$$q_t = -\frac{A_a}{\rho} \bar{p}_z - \frac{F}{\rho} q \quad (4.6)$$

$$q(0, t) = q_p(t) + q_i(t) \quad (4.7)$$

$$p(l, t) = p_c(t) \quad (4.8)$$

In order to transform the above PDE model of wellbore hydraulics Eq. (4.5) – (4.8) into the form of 2 x 2 linear hyperbolic system Eq. (4.1) – (4.4), which is needed for the observer design, we need to consider the following variable based on Riemann's coordinates

$$\bar{u}(z, t) = \frac{1}{2} \left( q(z, t) + \frac{A_a}{\sqrt{\beta\rho}} \bar{p}(z, t) \right) \quad (4.9)$$

$$\bar{v}(z, t) = \frac{1}{2} \left( q(z, t) - \frac{A_a}{\sqrt{\beta\rho}} \bar{p}(z, t) \right) \quad (4.10)$$

The time-derivative of Eq. (4.9) and (4.10) is given by

$$\bar{u}_t = \frac{1}{2} \left( q_t(z, t) + \frac{A_a}{\sqrt{\beta\rho}} \bar{p}_t(z, t) \right) = -\sqrt{\frac{\beta}{\rho}} \bar{u}_z - \frac{F}{2\rho} (\bar{u} + \bar{v}) \quad (4.11)$$

$$\bar{v}_t = \frac{1}{2} \left( q_t(z, t) - \frac{A_a}{\sqrt{\beta\rho}} \bar{p}_t(z, t) \right) = -\sqrt{\frac{\beta}{\rho}} \bar{v}_z - \frac{F}{2\rho} (\bar{u} + \bar{v}) \quad (4.12)$$

The boundary condition can be written as follows

$$\bar{u}(0, t) = \frac{1}{2} \left( q_p(t) + q_i(t) + \bar{u}(0, t) - \bar{v}(0, t) \right) = -\bar{v}(0, t) + q_p(t) + q_i(t) \quad (4.13)$$

$$\bar{v}(l, t) = \frac{1}{2} \left( (\bar{u}(l, t) + \bar{v}(l, t)) - \frac{A_a}{\sqrt{\beta\rho}} p_c(t) \right) = \bar{u}(l, t) - \frac{A_a}{\sqrt{\beta\rho}} p_c(t) \quad (4.14)$$

By defining

$$u(x, t) = \bar{u}(xl, t) e^{ax} \quad (4.15)$$

$$v(x, t) = \bar{v}(xl, t) e^{-ax} \quad (4.16)$$

with aforementioned transformation, the time and spatial derivatives of Eq. (4.15) is given by

$$u_t = -\sqrt{\frac{\beta}{\rho}}\bar{u}_z e^{ax} - \frac{F}{2\rho}(u(x,t) + v(x,t)e^{2ax}) \quad (4.17)$$

$$u_x(x,t) = l\bar{u}_z(xl,t)e^{ax} + a\bar{u}(xl,t)e^{ax} \quad (4.18)$$

so that

$$\bar{u}_z(xl,t) = \frac{1}{l}u_x(x,t)e^{-ax} - \frac{a}{l}u(x,t)e^{-ax} \quad (4.19)$$

By plugging Eq. (4.19) to (4.17), then

$$u_t = -\frac{1}{l}\sqrt{\frac{\beta}{\rho}}u_x(x,t) + \left(\frac{a}{l}\sqrt{\frac{\beta}{\rho}} - \frac{F}{2\rho}\right)u - \frac{F}{2\rho}e^{2ax}v(x,t) \quad (4.20)$$

By defining  $a = \frac{Fl}{2\sqrt{\beta\rho}}$ , and insert in Eq. (4.20) and the same for Eq. (4.16), we obtain the following equation

$$u_t = -\frac{1}{l}\sqrt{\frac{\beta}{\rho}}u_x(x,t) - \frac{F}{2\rho}e^{2ax}v(x,t) \quad (4.21)$$

$$v_t = \frac{1}{l}\sqrt{\frac{\beta}{\rho}}v_x(x,t) - \frac{F}{2\rho}e^{-2ax}u(x,t) \quad (4.22)$$

$$u(0,t) = -v(0,t) + q_p(t) + q_i(t) \quad (4.23)$$

$$v(1,t) = u(1,t)e^{-2a} - \frac{A_a e^{-a}}{\sqrt{\beta\rho}}p_c(t) \quad (4.24)$$

The equation above resembles to (4.1) to (4.4) with

$$\epsilon_1(x) = \epsilon_2(x) = \frac{1}{l}\sqrt{\frac{\beta}{\rho}} \quad (4.25)$$

$$c_1(x) = -\frac{F}{2\rho}e^{2ax} \quad (4.26)$$

$$c_2(x) = -\frac{F}{2\rho}e^{-2ax} \quad (4.27)$$



$$q = -1 \quad (4.28)$$

$$v_i(t) = q_p(t) \quad (4.29)$$

$$U(t) = u(1, t)e^{-2a} - \frac{A_a e^{-a}}{\sqrt{\beta\rho}} p_c(t) \quad (4.30)$$

The original state for the flow and pressure dynamics can be obtained as follows

$$q(z, t) = u\left(\frac{z}{l}, t\right) e^{-\frac{a}{l}z} + v\left(\frac{z}{l}, t\right) e^{\frac{a}{l}z} \quad (4.31)$$

$$p(z, t) = \frac{\sqrt{\beta\rho}}{A_a} \left( u\left(\frac{z}{l}, t\right) e^{-\frac{a}{l}z} - v\left(\frac{z}{l}, t\right) e^{\frac{a}{l}z} \right) + \rho g(l - z) \quad (4.32)$$

## 4.2 DISCRETIZATION

For pressure estimation scheme, the infinite dimensional systems of PDEs are discretized as a finite high-dimensional approximation in ODEs or known as the early lumping approach (Hasan, 2014). The method of lines is a numerical technique to solve PDEs in which only one dimension is discretized. Generally, in a time-dependent PDEs, the analysis of numerical methods can be done by first discretizing the spatial derivatives and leaving the time variable continuous. In this section, the spatial coordinate ( $x$ ) will be discretized for  $N$ -nodes. As a result, the linear hyperbolic system in Eq. (4.1) - (4.4) can be written into a lumped model. Therefore, the flow and pressure dynamics of the system in Eq. (4.31) and (4.32) can be expressed as a state space representation that can be solved by numerical solvers in the simulator. For  $i = \{1, \dots, N\}$ , equation (4.1) - (4.2) can be written as

$$\frac{du_i}{dt} = -\epsilon_1(x_i) \frac{du_i}{dx_i} + c_1(x_i)v_i \quad (4.33)$$

$$\frac{dv_i}{dt} = \epsilon_2(x_i) \frac{dv_i}{dx_i} + c_2(x_i)u_i \quad (4.34)$$

Using an upwind finite difference scheme, the definition of a derivative is given by

$$\frac{d}{dx} f(x_0) = \lim_{\Delta x \rightarrow 0} \frac{f(x_0) - f(x_0 - \Delta x)}{\Delta x} \quad (4.35)$$

Then the derivatives of Eq. (4.33) and (4.34) with respect to  $x$ , can be written as follows

$$\frac{du_i}{dx} = \frac{u_i - u_{i-1}}{\delta x} \quad (4.36)$$

$$\frac{dv_i}{dx} = \frac{v_{i+1} - v_i}{\delta x} \quad (4.37)$$

where  $\delta x = \frac{1}{N+1}$ . Due to the boundary conditions, the discretization scheme between  $u$  and  $v$  are slightly different.

Insert Eq. (4.36) - (4.37) to (4.33) - (4.34):

$$\frac{du_1}{dt} = -\epsilon_1(x_1) \frac{u_1 - u_0}{\delta x} + c_1(x_1)v_1 \quad (4.38)$$

$$\frac{du_2}{dt} = -\epsilon_1(x_2) \frac{u_2 - u_1}{\delta x} + c_1(x_2)v_2 \quad (4.39)$$

$$\frac{du_N}{dt} = -\epsilon_1(x_N) \frac{u_N - u_{N-1}}{\delta x} + c_1(x_N)v_N \quad (4.40)$$

$$\frac{dv_1}{dt} = \epsilon_2(x_1) \frac{v_2 - v_1}{\delta x} + c_2(x_1)u_1 \quad (4.41)$$

$$\frac{dv_2}{dt} = \epsilon_2(x_2) \frac{v_3 - v_2}{\delta x} + c_2(x_2)u_2 \quad (4.42)$$

$$\frac{dv_N}{dt} = -\epsilon_2(x_N) \frac{v_N - v_{N+1}}{\delta x} + c_2(x_N)u_N \quad (4.43)$$

By considering that  $v_1 \approx \frac{v_0 + v_2}{2}$ , then left boundary can be computed by interpolating  $v_0 \approx 2v_1 - v_2$  and as a result  $u_0 = q(2v_1 - v_2) + U_1$ . The ODEs of Eq. (4.38) - (4.43) can be written as a state-space representation, where a mathematical model in the first-order differential equation shown as a set of state variables, input, and output. The state-space representation is given by

$$\dot{x}(t) = Ax(t) + BU(t) \quad (4.44)$$

- $x$  is  $n \times 1$  ( $n$  rows by 1 column). It is the state vector and a function of time
- $A$  is  $n \times n$ . It is the state matrix
- $B$  is  $n \times r$ . It is the input matrix

- $U$  is  $r \times 1$ . It is the input as a function of time. In practice, it is the representation of the input from the choke pressure over time

The state of the system is represented as a vector within a space whose axes, in this case  $x$ , is the state variable. The state vector ( $x$ ) can be written as

$$x = [u_1 \dots u_N \quad v_1 \dots v_N]^T \quad (4.45)$$

The state matrix ( $A$ ) is given by

$$A = \begin{pmatrix} E_1 & C_1 \\ C_1 & E_2 \end{pmatrix} \quad (4.46)$$

where

$$C_1 = \text{diag}(c_1) + \begin{pmatrix} 2q \frac{\epsilon_1(x_1)}{\delta x_1} & -q \frac{\epsilon_1(x_1)}{\delta x_1} & 0 \\ 0 & 0 & 0 \end{pmatrix}, \quad (4.47)$$

$$C_2 = \text{diag}(c_2), \quad (4.48)$$

$$E_1 = \frac{1}{\delta x} \begin{pmatrix} -\epsilon_1(x_1) & 0 & \dots & 0 \\ \epsilon_1(x_2) & -\epsilon_1(x_2) & \dots & 0 \\ \vdots & \vdots & \ddots & \vdots \\ 0 & 0 & \dots & -\epsilon_1(x_N) \end{pmatrix}, \quad (4.49)$$

$$E_2 = \frac{1}{\delta x} \begin{pmatrix} -\epsilon_2(x_1) & \epsilon_2(x_1) & \dots & 0 \\ 0 & -\epsilon_2(x_2) & \dots & 0 \\ \vdots & \vdots & \ddots & \vdots \\ 0 & 0 & \dots & -\epsilon_2(x_N) \end{pmatrix}, \quad (4.50)$$

The input matrix ( $B$ ) is given by

$$B = \frac{1}{\delta x} \begin{pmatrix} \epsilon_1(x_1) & 0 \\ 0 & -\epsilon_2(x_N) \end{pmatrix} \quad (4.51)$$

while the input can be defined as follows

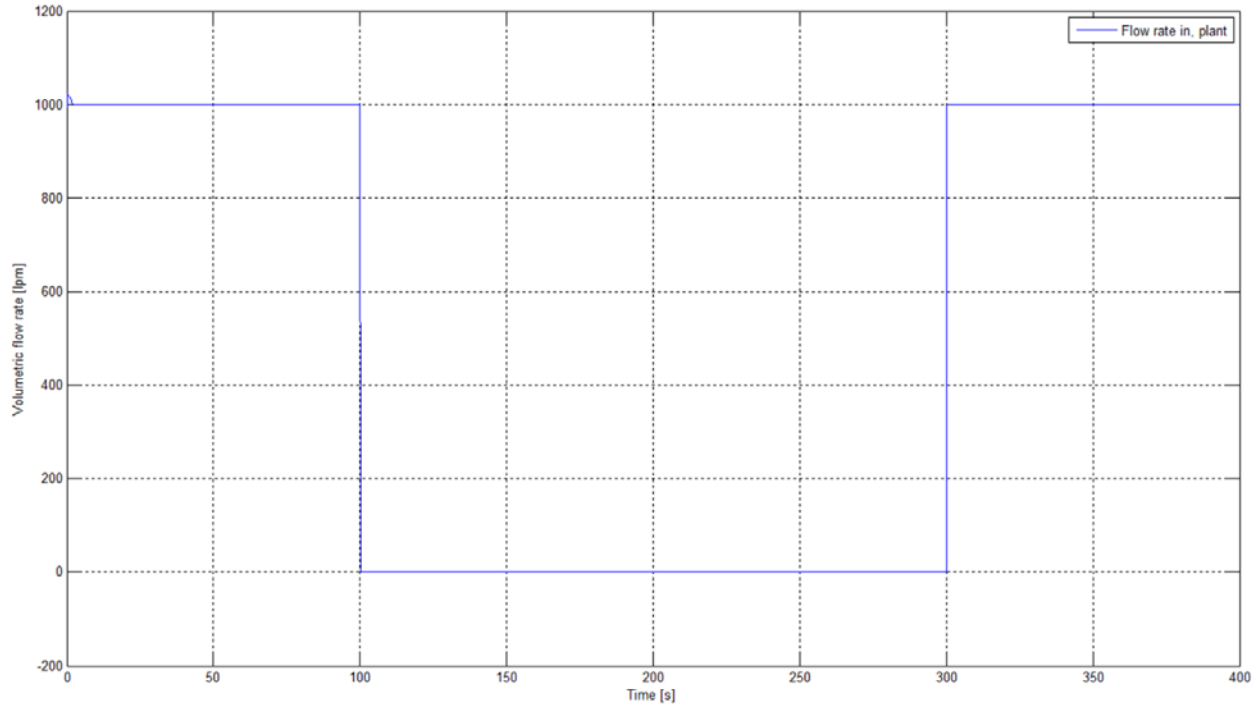
$$U = \begin{pmatrix} U_1 \\ U_2 \end{pmatrix} \quad (4.52)$$

### 4.3 SIMULATION

In this section, the simulation is performed to consider the use of the hydraulic model in 2 x 2 linear hyperbolic system. It simulates the dynamics of the hydraulic system during drilling connection using MATLAB (Appendix A). The depth of the vertical well is 2000m and the flow rate of the main pump is 1000lpm. In the case of drilling connection, the main circulation will be stopped by turning off the main pump at 100 seconds, and by the time the drilling connection procedure finish at 300 seconds, the main pump is turned back on to initial flow rate of 1000lpm before the drilling operation proceeds. The numerical values used for the physical parameters are given in Table 4.1

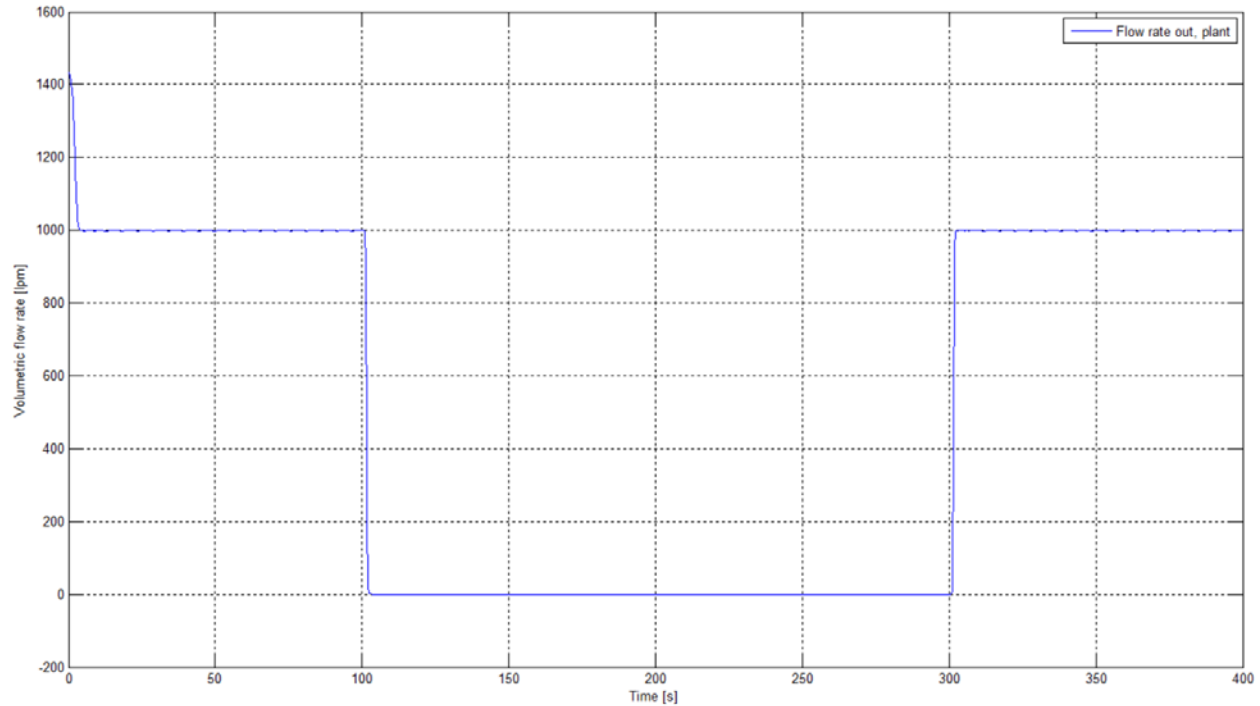
**Table 4.1: Wellbore Parameters for Simulation of Drilling Connection**

<b>Parameter</b>	<b>Description</b>	<b>Value</b>	<b>Unit</b>
$\beta$	Bulk modulus	$2 \times 10^9$	$Pa$
$A_a$	Annulus cross sectional area	0.03	$m^2$
$A_d$	Drillstring cross sectional area	0.006	$m^2$
$F$	Friction factor	1	$kg/m^3$
$g$	Gravity constant	9.81	$m/s^2$
$\rho$	Mud density	1250	$kg/m^3$



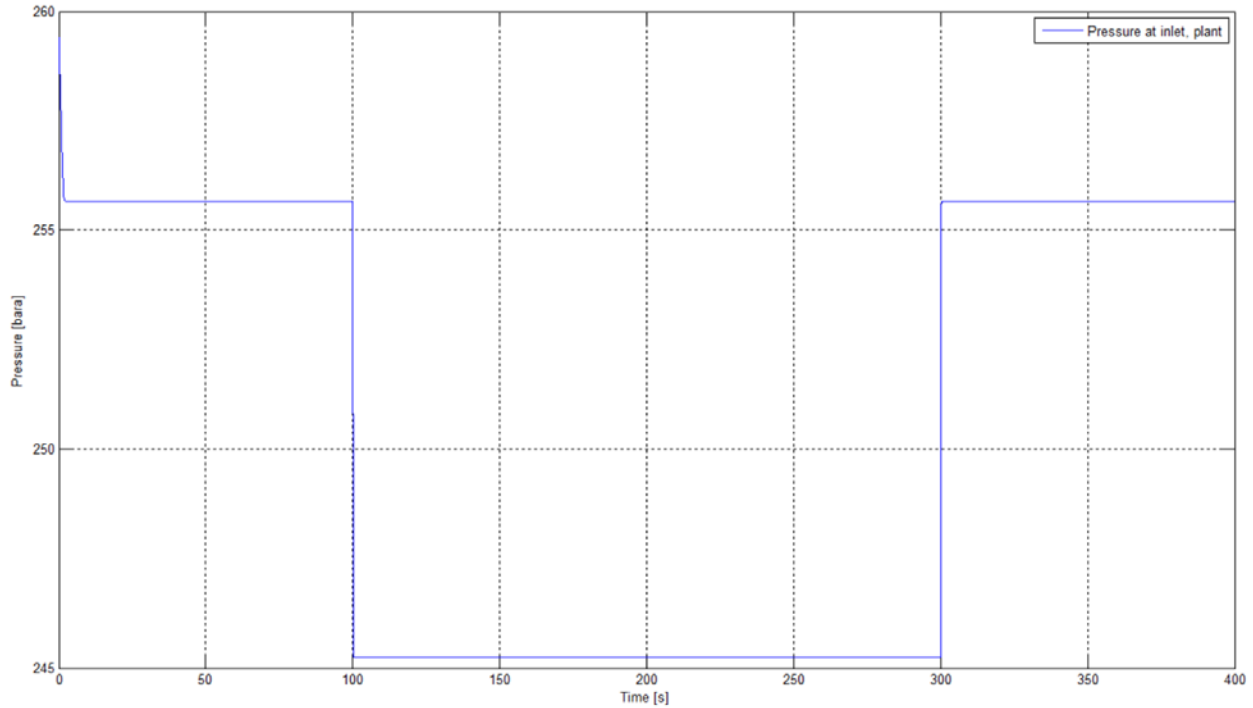
**Figure 4.2: Flowrate at the Inlet (Bottomhole)**

Figure 4.2 shows the dynamics of the flow in the bottomhole. It shows that at  $t=100s$ , the main circulation is stopped from 1000lpm to 0lpm by turning off the main pump, in order to prepare for making up connection. After making up connection finish at  $t=300s$ , the flow rate is turned back on to 1000lpm, in order to continue a drilling operation.



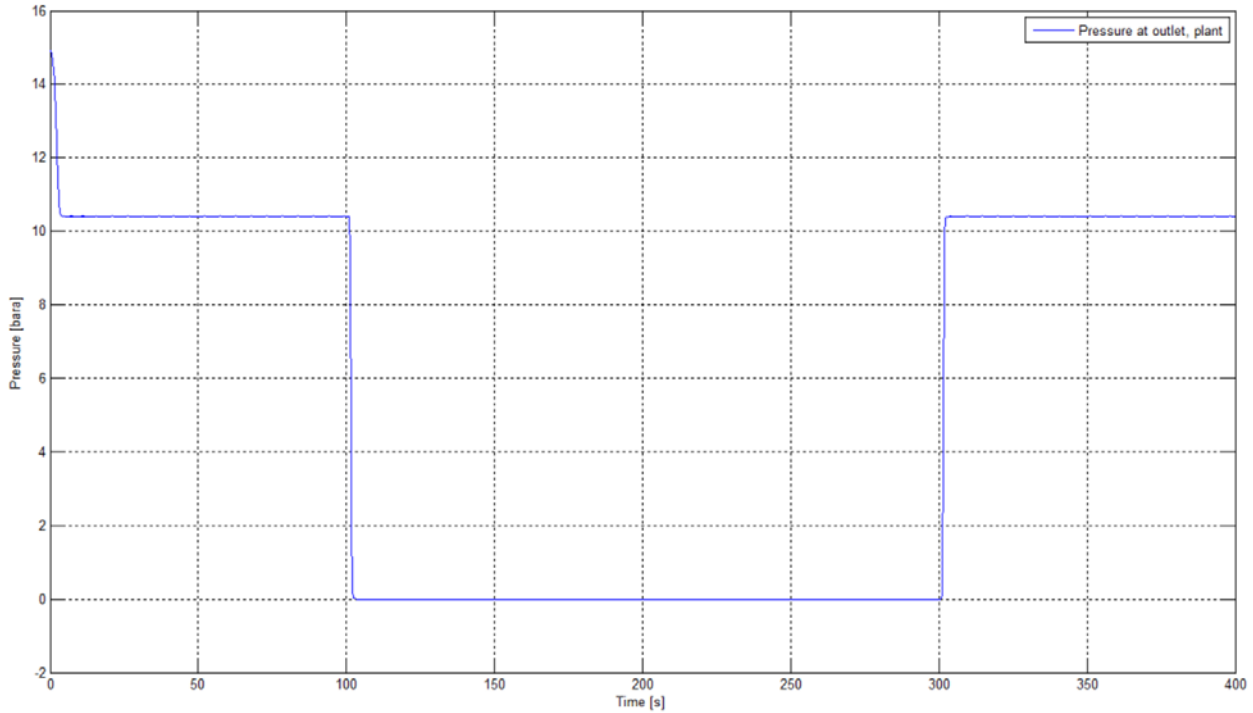
**Figure 4.3: Flowrate at the Outlet (Choke)**

Figure 4.3 shows the dynamics of the flow in the topside (choke). It shows few seconds of delay compared to the flow dynamics on the bottomhole in Figure 4.1. This figure shows that the effect of turning off and turning on the flow rate of the main pump can be seen in the topside few seconds after it effects the flow dynamics in the bottomhole. The flowrate is going down from 1000lpm to 0lpm at 103s and is going up to 1000lpm again at 303s.



**Figure 4.4: Pressure at the Inlet (Bottomhole)**

Figure 4.4 shows the pressure dynamics in the bottomhole. It shows that at  $t=100\text{s}$ , the bottomhole pressure is going down because the flow rate from the main pump is turned off in order to prepare for making up connection. The reduction of bottomhole pressure from 256bara down to 245.5bara is because of the loss of frictional pressure along the annulus of the wellbore, and loss of backpressure from the choke as shown in Figure 4.5. The pressure is stable at 245.5bara due to the hydrostatic pressure from the drilling fluid ( $1250\text{ kg/m}^3$ ) in the annulus. After making up connection finish at  $t=300\text{s}$ , the flow rate is turned back on to 1000lpm. As a result, the bottomhole pressure is back at 256bara.



**Figure 4.5: Pressure at the Outlet (Choke)**

Figure 4.5 shows the pressure dynamics in the topside (choke). It shows few seconds of delay compared to the pressure dynamics on the bottomhole. This figure shows that the effect of turning off and turning on the flow rate of the main pump can be seen in the topside few seconds after it effects the pressure dynamics in the bottomhole. The choke pressure is initially maintained at 10.5 bara before going down to 0bara during the start of connection at 103s, and the choke pressure is back at 10.5 bara at  $t=303s$  to continue drilling operation.

These simulations show that the hydraulics in MPD system can be modeled in  $2 \times 2$  linear hyperbolic PDEs. The result from numerical simulation of shows that the pressure and flow dynamics during drilling connection can be computed by using the hydraulic model that has been transformed into a linear hyperbolic system, and it shows a proper relation between turning off and turning on the main pump during connection to the bottomhole pressure, choke pressure, and choke flowrate. In the following chapter, an adaptive observer will be outlined and the numerical simulation will be performed to compare the observer with the actual pressure and flow dynamics that has been simulated in this chapter.



## 5. ADAPTIVE OBSERVER DESIGN

In a drilling operation, the downhole measurements are typically less reliable than the topside measurements due to slow sampling, transmissions delays, and loss of communication for low or no-flow conditions. Therefore, the measured volumetric flow and pressure from the flow meter and the pressure gauge at the topside of the well are considered as the only reliable measurement during drilling. Since the downhole pressure is the variable to control in MPD operation, an adaptive observer or parameter estimation scheme is required to accurately estimate the downhole pressure based on the measurement at the surface.

An adaptive observer design based on backstepping method is presented in this chapter. The backstepping method is a systematic method for control and estimation problems of distributed parameter systems that have been used successfully for state and parameter estimation of many types of PDEs. It allows the design of boundary control laws, boundary observers and output-feedback control laws, which guarantee the stability of the closed-loop system and convergence of the state estimates. The design, which is based on Volterra integral transformation relies only on a measurement at the right boundary of the system (topside), and the observer gains are obtained by solving a first-order hyperbolic system of Goursat-type PDEs (Hasan, 2015). This solution to the Goursat system is related to the solution of a simpler, explicitly solvable Goursat system through a suitable infinite series of powers of partial derivatives which is summed explicitly in terms of special functions, such as Bessel functions and the generalized Marcum Q-functions of the first order (Vazquez et al, 2013).

In practice, the observer can be used to accurately estimate the downhole pressure, flow dynamics and the unknown parameter such as fluid loss using only on measurement at the topside. Numerical simulations of drilling events such as drilling connection and lost circulation are also presented in this chapter to examine the accuracy of the observer for the estimation of downhole pressure, the rate of lost circulation and another unknown parameter. In addition, analysis from Lyapunov approach is outlined to investigate the convergence of the estimation error.

## 5.1 STATE AND PARAMETER ESTIMATION

The main objective of an adaptive observer is to estimate unmeasured states in a dynamic system with parametric uncertainties. In most MPD operation, the pressure profile throughout the wellbore is not measured and the data quality for feedback control is low due to the noise, slow sampling rates and loss of communication. Due to the lack of measurement for the control purposes, an estimation scheme for pressure and flow dynamics of the wellbore is important for control design in MPD system. In addition to estimating the pressure and flow dynamics, an adaptive observer can also be used to estimate parameter uncertainties such as friction, influx, and fluid loss. These unmeasured data can be estimated by adjusting the dynamic system based on the available measurement at topside (Stamnes, 2011).

The estimation of the dynamic system using deterministic approach is called as an observer, while the estimation of the dynamic system using stochastic approach is called filter or an estimator as discussed in Kalman (1960). An observer is mainly used to estimate the dynamic system while the parameters are well-known. On the other hand, an adaptive observer is useful in the case of uncertain parameters in the system. As in the case of MPD, there are uncertain parameters such as friction, influx and fluid loss that need to be accurately estimated in order to have accurate estimation of the state system, that is pressure dynamics of the wellbore.

The current adaptive observer design does not cover the linear hyperbolic system to which the hydraulic model has been transformed in this work. Therefore, an adaptive observer design for this specific class of linear hyperbolic system is presented in this chapter. The adaptive observer is based on a backstepping method that guarantees stability and convergence of the state estimation.

### 5.1.1 Adaptive Observer

This section provides an introduction to the adaptive observer. The observer provides an estimation the downhole pressure and the unknown parameter (friction) in the annulus. The detail presented below is based on the linear time varying model (Stamnes, 2007) and it serves only as an introduction to the adaptive observer design. Meanwhile, the main topic of this work, that is adaptive observer design based on a linear hyperbolic system will be outlined in the next section, Chapter 5.2 and 5.3.

Consider linear systems as follows

$$\dot{x} = Ax + Bu \quad (5.1)$$

$$y = Cx \quad (5.2)$$

where  $x$  is the state,  $u$  is the measured input and  $y$  is the measurements ( $\Delta p_{bit}$ ). Due to the presence of uncertain parameters in the hydraulic model, then an adaptive observer is designed for state and parameter estimation. In many cases, the unknown parameter is represented by introducing  $\theta$ , and multiply it by a measured function.

$$\dot{x} = Ax + Bu + \phi(t)\theta \quad (5.3)$$

$$y = Cx \quad (5.4)$$

where

$$A(t) = \begin{bmatrix} 0 & 0 & a_{13} \\ 0 & 0 & a_{23} \\ a_{31} & -a_{31} & a_{33} \end{bmatrix} \quad (5.5)$$

$$B(t) = \begin{bmatrix} b_{11} & 0 \\ 0 & b_{22} \\ 0 & 0 \end{bmatrix} \quad (5.6)$$

$$C(t) = \begin{bmatrix} c_1 \\ c_2 \\ c_3 \end{bmatrix}^T \quad (5.7)$$

where  $x_1$  and  $x_2$  are measured.  $a_{33}$  is dependent on the estimated unknown parameter,  $F_a$ , therefore  $\theta = a_{33}$  and it is estimated by  $\hat{\theta}$ .

### 5.1.2 Error Dynamics

The dynamics of  $\xi$ , can be written as

$$\dot{\xi} = \Delta\dot{x}_3 + l_1\Delta\dot{x}_1 \quad (5.8)$$

$$\dot{\xi} = a_{31}\Delta x_1 - a_{31}\Delta x_2 + (\theta + l_1 a_{13})\Delta x_3 + l_1 b_{11}\Delta u_1 \quad (5.9)$$

An observer of  $\Delta x_3$  is given by

$$\Delta\hat{x}_3 = \dot{\xi} - l_1\Delta x_1 \quad (5.10)$$

The dynamics of the estimation error can be found as

$$\Delta\tilde{x}_3 = \Delta x_3 - \Delta\hat{x}_3 = \xi - \hat{\xi} = \tilde{\xi} \quad (5.11)$$

$$\tilde{\xi} = \xi - \hat{\xi} = \theta\Delta x_3 - \hat{\theta}\Delta\hat{x}_3 + l_1 a_{13}\Delta\tilde{x}_3 \quad (5.12)$$

Since  $\theta\Delta x_3 - \hat{\theta}\Delta\hat{x}_3 = \theta\Delta x_3 - \theta\Delta\hat{x}_3 + \theta\Delta\hat{x}_3 - \hat{\theta}\Delta\hat{x}_3 = \theta\Delta\tilde{x}_3 + \tilde{\theta}\Delta\hat{x}_3$ , then the dynamics of the estimation error can be written as follows

$$\tilde{\xi} = \theta\Delta\tilde{x}_3 + \tilde{\theta}\Delta\hat{x}_3 + l_1 a_{13}\Delta\tilde{x}_3 = (\theta + l_1 a_{13})\tilde{\xi} + \tilde{\theta}\Delta\hat{x}_3 \quad (5.13)$$

### 5.1.3 Lyapunov Analysis

The Lyapunov function is given by

$$\theta(\tilde{\xi}, \tilde{\theta}) = \frac{1}{2}\tilde{\xi}^2 + \frac{1}{2\gamma}\tilde{\theta}^2 \quad (5.14)$$

$$\frac{\partial V}{\partial t} = \tilde{\xi}\dot{\tilde{\xi}} + \frac{1}{\gamma}\dot{\tilde{\theta}} = \left((\theta + l_1 a_{13})\tilde{\xi}^2\right) + \tilde{\theta}(\Delta\hat{x}_3\tilde{\xi} + \frac{1}{\gamma}\dot{\tilde{\theta}}) \quad (5.15)$$

The dynamics of parameter estimation error can be found as

$$\dot{\tilde{\theta}} = -\gamma\Delta\hat{x}_3\tilde{\xi} \quad (5.16)$$

Assuming the parameter estimation error is slowly changes, then  $\dot{\tilde{\theta}} = 0$ . Then Lyapunov function, can be written as

$$\dot{V} = (\theta + l_1 a_{13})\tilde{\xi}^2 \quad (5.17)$$

By choosing  $l_1$  to satisfy  $(\theta + l_1 a_{13}) \leq 0$ , then the solution that is uniformly bounded can be found as follows

$$\lim_{t \rightarrow \infty} (\theta + l_1 a_{13})\tilde{\xi}^2 = 0 \quad (5.18)$$

## 5.2 ERROR DYNAMICS

This section present the adaptive observer design for hydraulic model in linear hyperbolic system that has been presented in Chapter 4. A thorough derivation of the observer design can be found in (Hasan, 2014). In the previous chapter, Eq. (4.21) – (4.24) shows that the physical system of wellbore hydraulic can be expressed by the following 2 x 2 linear hyperbolic system

$$w_t(x, t) = \Sigma(x)w_x(x, t) + C(x)w(x, t) \quad (5.19)$$

$$u(0, t) = qv(0, t) + v_p + \theta \quad (5.20)$$

$$v(1, t) = U(t) \quad (5.21)$$

where  $w = \begin{pmatrix} u \\ v \end{pmatrix}$ ,  $\Sigma = \begin{pmatrix} -\epsilon_i(x) & 0 \\ 0 & \epsilon_2(x) \end{pmatrix}$  and the matrix  $C(x) = \begin{pmatrix} 0 & c_1(x) \\ c_2(x) & 0 \end{pmatrix}$

An observer for  $w_t(x, t)$ , where  $u(1, t)$  is measured at the boundary

$$\widehat{w}_t = \Sigma(x)\widehat{w}_x + C(x)\widehat{w} + p(x)\tilde{u}(1, t) \quad (5.22)$$

$$\widehat{u}(0, t) = q\widehat{v}(0, t) + v_p + \widehat{\theta}(t) \quad (5.23)$$

$$\widehat{v}(1, t) = U(t) \quad (5.24)$$

where  $p(x) = [p_1(x) \ p_2(x)]^T$  is the observer gain to be determined later by solving a first-order hyperbolic system of Goursat-type PDEs.

From Eq. (5.19) and (5.22), Eq. (5.20) and (5.23), also Eq. (5.21) and (5.24), we have  $\tilde{u} = u - \widehat{u}$ ,  $\tilde{v} = v - \widehat{v}$  and  $\tilde{\theta} = \theta - \widehat{\theta}$ , then the dynamics of the state estimation error becomes:

$$\tilde{w}_t = \Sigma(x)\tilde{w}_x + C(x)\tilde{w} - p(x)\tilde{u}(1, t) \quad (5.25)$$

$$\tilde{u}(0, t) = q\tilde{v}(0, t) + v_p + \tilde{\theta}(t) \quad (5.26)$$

$$\tilde{v}(1, t) = 0 \quad (5.27)$$

In Aamo (2013), the coordinate transformation Eq. (4.1) – (4.2) decoupling into a subsystem, by using the infinite-dimensional backstepping transformation. In the case of  $\theta = 0$ , then the backstepping method to control the linear PDEs with Volterra nonlinearities is given by

$$\tilde{w}(x, t) = \tilde{\gamma}(x, t) - \int_x^1 P(x, \xi)\tilde{\gamma}(\xi, t) d\xi \quad (5.28)$$

where  $\tilde{\gamma} = \begin{pmatrix} \tilde{\alpha} \\ \tilde{\beta} \end{pmatrix}$  and  $P = \begin{pmatrix} P^{uu} & P^{uv} \\ P^{vu} & P^{vv} \end{pmatrix}$  is the transformation kernel. The target system will be exponentially stable and converge to the true values by using  $\tilde{\gamma} = [\alpha \ \beta]^T$ . The transformation kernel  $P^{vu}$  and  $P^{vv}$  from Eq. (5.28) are the solutions to the following system of PDEs

$$\varepsilon_1(x)P_x^{uu} + \varepsilon_1(\xi)P_\xi^{uu} = -\varepsilon'_1(\xi)P^{uu} - c_1(x)P^{vu} \quad (5.29)$$

$$\varepsilon_1(x)P_x^{uv} - \varepsilon_2(\xi)P_\xi^{uv} = \varepsilon'_2(\xi)P^{uv} - c_1(x)P^{uv} \quad (5.30)$$

$$\varepsilon_2(x)P_x^{vu} - \varepsilon_1(\xi)P_\xi^{vu} = \varepsilon'_1(\xi)P^{vu} + c_2(x)P^{uu} \quad (5.31)$$

$$\varepsilon_2(x)P_x^{vv} + \varepsilon_2(\xi)P_\xi^{vv} = -\varepsilon'_2(\xi)P^{uv} + c_2(x)P^{uv} \quad (5.32)$$

defined over the triangular domain  $T = \{(x, y): 0 \leq y \leq x \leq 1\}$  with boundary condition

$$P^{uu}(0, \xi) = qP^{vu}(0, \xi) \quad (5.33)$$

$$P^{uv}(x, x) = \frac{c_1(x)}{\varepsilon_1(x) + \varepsilon_2(x)} \quad (5.34)$$

$$P^{vu}(x, x) = -\frac{c_2(x)}{\varepsilon_1(x) + \varepsilon_2(x)} \quad (5.35)$$

$$P^{vv}(0, \xi) = \frac{1}{q}P^{vu}(0, \xi) \quad (5.36)$$

The control kernels above are given in terms of modified Bessel functions, and also in terms of the generalized Marcum Q-function of the first order. Backstepping transformation is used to derive the explicit solutions. The kernels used in the feedback law are found by solving a 2 x 2 linear hyperbolic PDEs in a triangular domain (known as kernel equations). When the plant model has a constant coefficient, the resulting kernel equations have a very specific structure which can be exploited to obtain an explicit solution in terms of special functions (Vazquez et al, 2013).

The unknown parameter such as fluid loss will be estimated by introducing an update-law ( $\theta$ ) and using backstepping method in Eq. (5.28), then equation Eq. (5.25) – (5.27) will be transformed as follows

$$\tilde{y}_t = \sum x (\tilde{y}_x) + \bar{p}\alpha(1, t) \quad (5.37)$$

$$\tilde{\alpha}(0, t) = q\tilde{\beta}(0, t) + \tilde{\theta}(t) \quad (5.38)$$

$$\tilde{\beta}(1, t) = 0 \quad (5.39)$$

where  $\bar{p} = [-\kappa \ 0]^\tau$  and  $\beta$  is exponentially stable. The explicit expression for observer gains  $p_1(x)$  and  $p_2(x)$  from the first-order hyperbolic system of Goursat-type PDEs can be obtained as

$$p_1(x) = \kappa - \varepsilon_1(1)P^{uu}(x, 1) - \int_x^1 \kappa P^{uu}(x, \xi) d\xi \quad (5.40)$$

$$p_2(x) = -\varepsilon_1(1)P^{vu}(x, 1) - \int_x^1 \kappa P^{vu}(x, \xi) d\xi \quad (5.41)$$

Consider  $\alpha$  to check if Eq. (5.19) – (5.21) is exponentially stable

$$\tilde{\alpha}_t(x, t) = -\varepsilon_1(x)\tilde{\alpha}_x(x, t) - \kappa\tilde{\alpha}(1, t) \quad (5.42)$$

$$\tilde{\alpha}(0, t) = \tilde{\theta}(t) \quad (5.43)$$

By defining  $\tilde{\phi}(x, t) = \tilde{\alpha}(x, t) - \tilde{\theta}(t)$ , and  $\tilde{\phi}_t(x, t) + \varepsilon_1(x)\tilde{\phi}_x(x, t) = \tilde{\alpha}_t(x, t) - \tilde{\theta}(t) + \varepsilon_1(x)\tilde{\alpha}_x(x, t)$ , then the update law for parameter estimation is given by

$$\tilde{\theta}(t) = \kappa\tilde{\alpha}(1, t) \quad (5.44)$$

for  $\kappa > 0$ . The  $\tilde{\phi}$  can be expressed as:

$$\tilde{\phi}(x, t) = -\varepsilon_1(x)\tilde{\phi}_x(x, t) \quad (5.45)$$

$$\tilde{\phi}(x, t) = 0 \quad (5.46)$$

The error for the update law is given as follows

$$\tilde{\theta}(t) = -\kappa\tilde{\phi}(1, t) - \kappa\tilde{\theta}(t) \quad (5.47)$$

### 5.3 CONVERGENCE OF ESTIMATED STATE ( $\hat{\omega}$ ) AND PARAMETER ( $\tilde{\theta}$ )

The stability of the system will be found from Lyapunov function as shown in Eq. (5.14). The Lyapunov function used for this system is given by

$$V(t) = \frac{1}{2} \tilde{\theta}(t)^2 + c \int_0^1 \frac{2-x}{\varepsilon_1(x)} \tilde{\phi}(x, t)^2 dx \quad (5.48)$$

where  $c > 0$ . Computing its time derivative along Eq. (5.45), (5.46), and (5.47) using integration by parts yields

$$\dot{V}(t) = -\kappa \tilde{\theta}(t)^2 - \kappa \tilde{\phi}(1, t) \tilde{\theta}(t) - c \tilde{\phi}(1, t)^2 - c \int_0^1 \tilde{\phi}(x, t)^2 dx \quad (5.49)$$

where  $c > 0$ . Since  $\bar{u}(1, t) = \tilde{\theta}(t)$ , then

$$\frac{\kappa}{2} \tilde{\theta}(t)^2 + \kappa \tilde{\phi}(1, t) \tilde{\theta}(t) + c \tilde{\phi}(1, t)^2 \geq 0 \quad (5.50)$$

$$\dot{V}(t) = -\frac{\kappa}{2} \tilde{\theta}(t)^2 - c \int_0^1 \tilde{\phi}(x, t)^2 dx \quad (5.51)$$

As time derivative of the Lyapunov function Eq. (5.51) has negative real parts, then Eq. (5.37) – (5.39) is exponentially stable in the following term.

$$\left( \tilde{\theta}(t)^2 + \int_0^1 \tilde{\alpha}(x, t)^2 dx + \int_0^1 \tilde{\beta}(x, t)^2 dx \right) \quad (5.52)$$

In Vazquez et al. (2013), the proof of existence and uniqueness of solutions Eq. (5.29) – (5.32) and Eq. (5.33) – (5.36) were outlined, and it was also proved that the solutions are continuous over  $T$ . The stability of Eq. (5.37) – (5.39) can be converted into the stability of the state estimation error Eq. (5.37) – (5.39) because the transformation using backstepping method Eq. (5.28) is invertible. As a result, the state estimation  $\hat{\omega}$  and parameter estimation  $\tilde{\theta}$  converge exponentially to the true values of  $u$ ,  $v$ , and  $\theta$ .

### 5.4 SIMULATION

There are several operational procedure and drilling problems during MPD operation that affect the downhole pressure. One of the most common procedure in drilling operation is pipe connection, that



is a procedure where once the bit on the bottom has drilled down to where the topdrive at the top reach the drillfloor, approximately 90ft, then a new stand of pipe is again connected to the topdrive. In order to connect the new stand to the drillstring, the mud circulation need to be stopped by ramping down the main pump flow. Once the procedure for making up new stand is completed then the main pump flow is ramped back up to the required flow rate for drilling the formation. The procedure for pipe connection affects the downhole pressure due to the loss of frictional pressure along the annulus as the main pump flow is ramped down to zero flow to attach new stand of drillpipe.

On the other hand, lost circulation is the situation of uncontrolled flow of mud into the formation. It might happen due to the natural or induced causes. The natural causes include scenario of drilling into zones which are highly permeable, cavernous, and inherently fractured. Induced losses occur when the wellbore pressure exceeds the fracture pressure of formation. As a result, there will be a fracture opening that leads to loss circulation. In the case of total loss returns where no fluid comes out of the annulus, the wellbore may not remain full of fluid. As a result, the fluid column drops and pressure exerted on the formation is reduced, which might allow an influx of formation fluid that could lead into a catastrophic loss of well control. Therefore, estimating and controlling lost circulation is an important issue in drilling operation.

The flow and pressure dynamics of the MPD system in Eq. (3.16) – (3.17) has been expressed in a state space representation which is convenient in order to utilize the numerical solvers included in MATLAB. The hydraulic model is solved by using MATLAB solver ode23. Using the adaptive observer presented in Eq. (5.22) – (5.24), where an uncertain parameter is estimated using the update law Eq. (5.47), the downhole pressure and the unknown parameter such as rate of lost circulation will be estimated in the following section

### **Case 1: Drilling Connection**

The simulation of adaptive observer for pressure and flow dynamics estimation during pipe connection will be based on the result of plant simulation in Chapter 4.3. The estimation of pressure and flow dynamics from the observer will be compared to the result from plant simulation or measurement in order to verify the capability of observer to accurately estimate the pressure and flow dynamics in the hydraulic system of MPD operations using only one measurement at the

boundary (topside) . The numerical values used for the simulation of pipe connection are similar with physical parameter presented in Table 4.1.

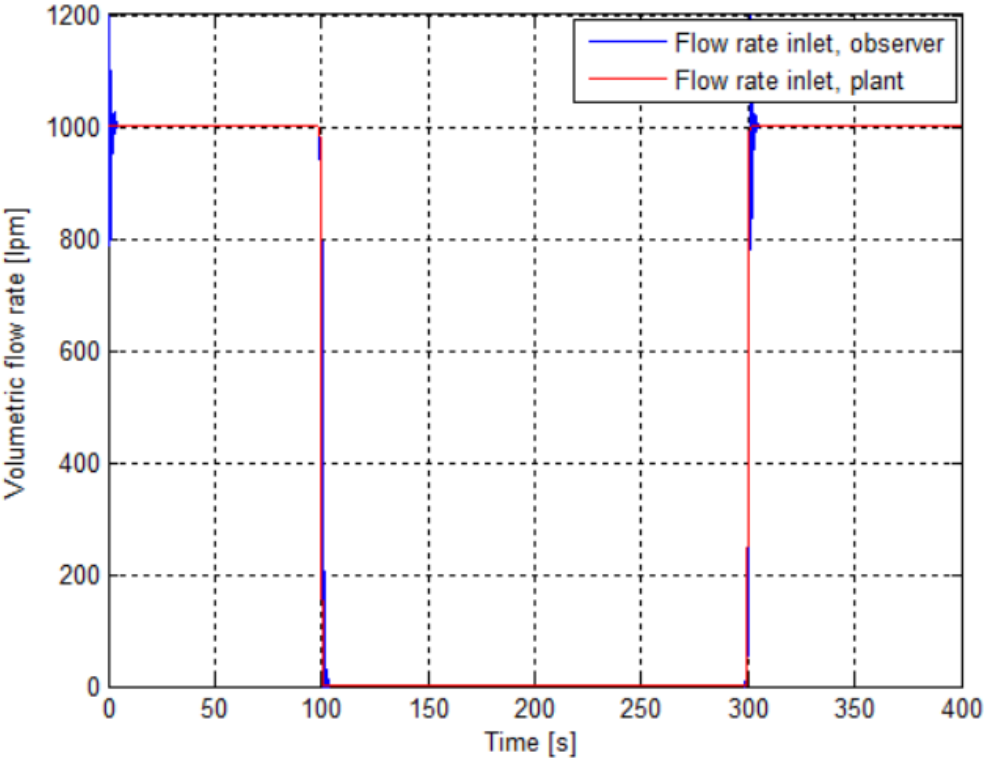


**Figure 5.1: Flowrate at the Inlet (Bottomhole)**

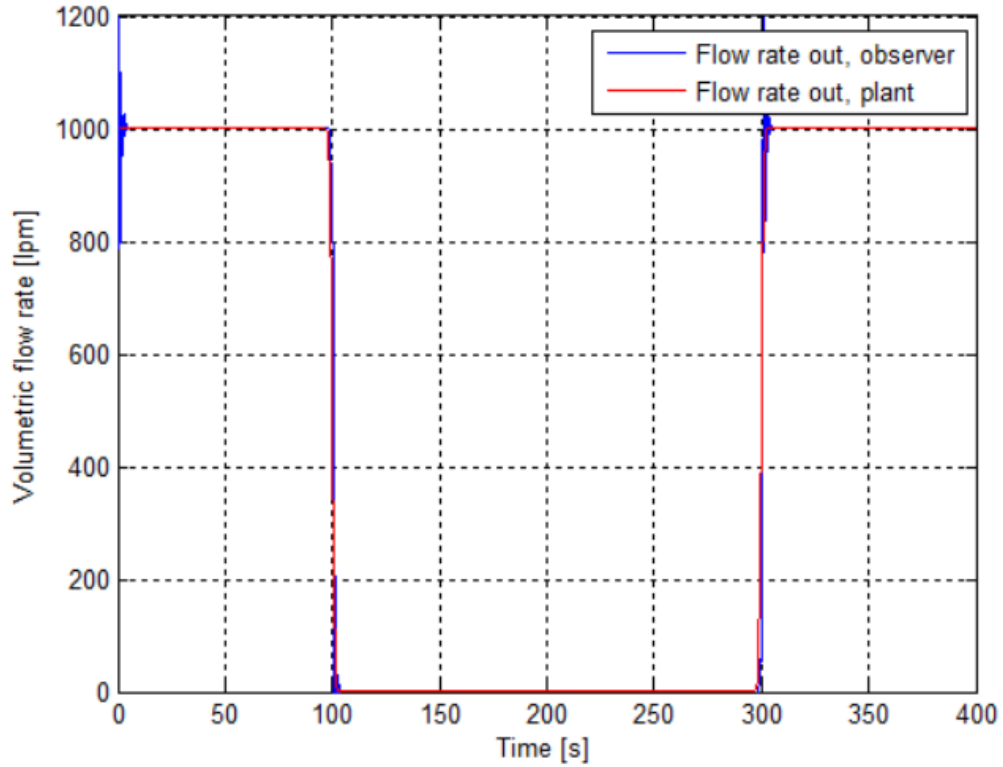


**Figure 5.2: Flowrate at the Outlet (Choke)**

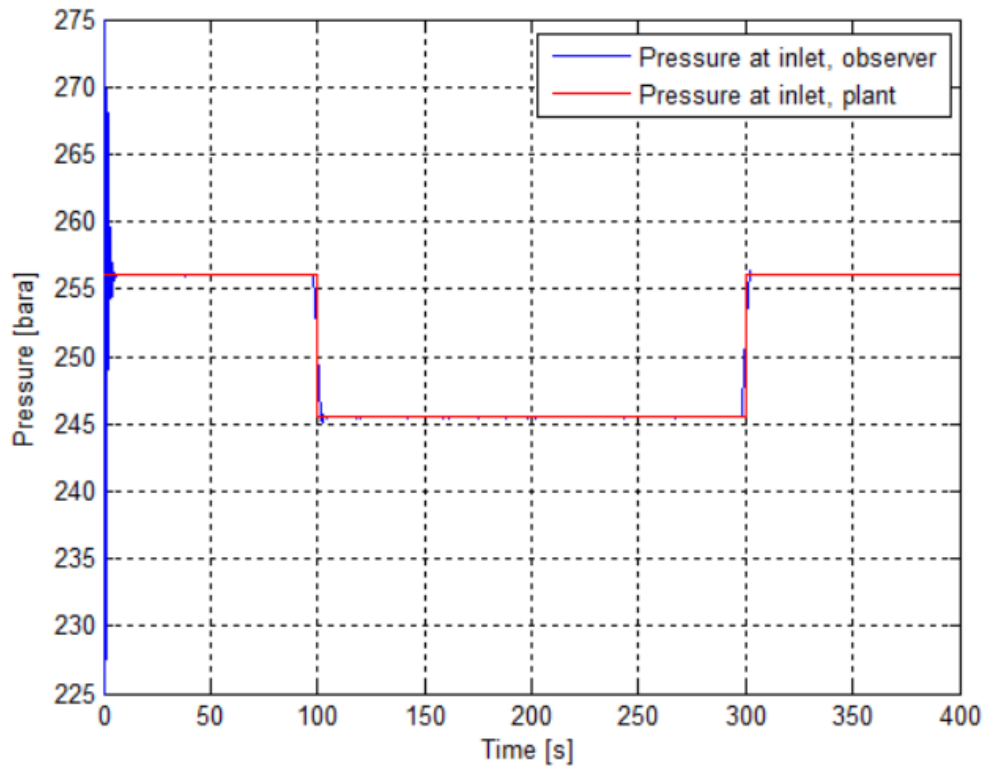


**Figure 5.3: Pressure at the Inlet (Bottomhole)**

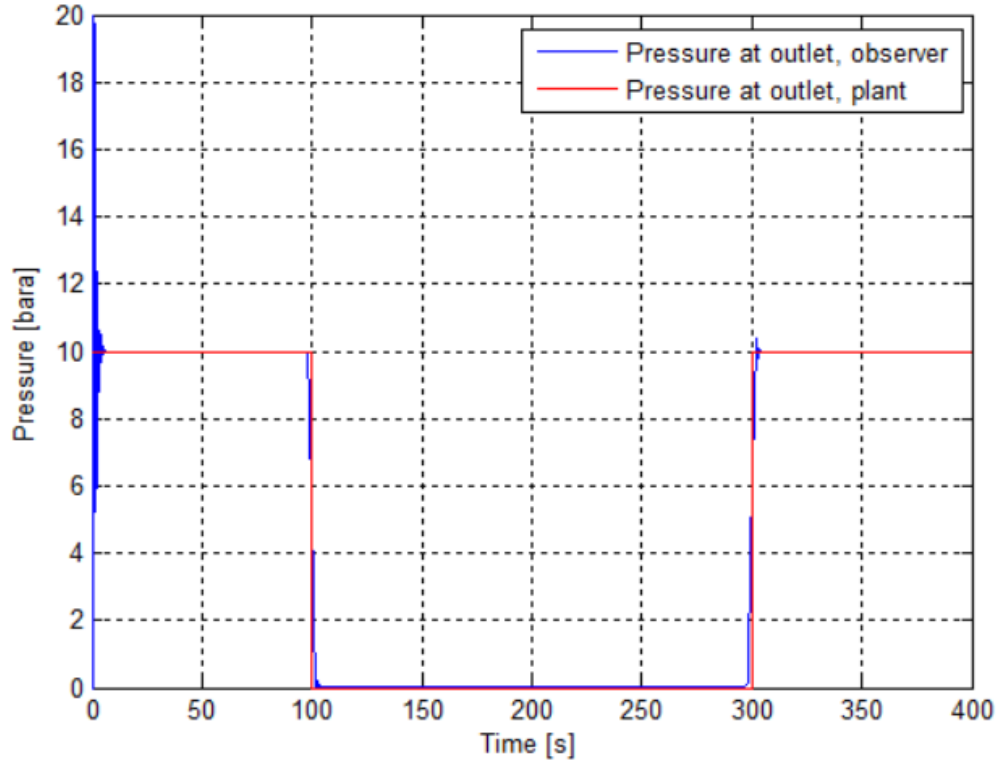


**Figure 5.4: Pressure at the Outlet (Choke)**

Figure 5.1 shows that at  $t=100s$ , the main pump is ramped down from 1000lpm to 0lpm. It leads to the loss of frictional pressure in the annulus and consequently the downhole pressure. Figure 5.3 shows the reduction of bottomhole pressure from 256bara down to its Equivalent Static Density (ESD) of 245.5bara. After  $t=300s$ , the main pump is ramped up back to 1000lpm and as a result the downhole pressure is back to 256bara. In this case, it is assumed that there is no influx from or outflux into the formation, therefore the flowrate profile at the choke manifold, Figure 5.2, follow the flowrate profile in the downhole. The choke pressure is initially maintained at 10.5bara before going down to 0bara during the start of connection, and the choke pressure is back at 10.5 bara at  $t=300s$  to continue drilling operation.

Figure 5.1 – 5.4 shows that the observer (blue lines) converge to the true values (red lines) that has been simulated in previous chapter, Figure 4.2 – 4.5. It can be concluded that the adaptive observer can accurately estimate the system state and the unknown parameter during drilling connection procedure. The discrepancy at the beginning of the simulation is a result of the observer being initialized with values different from the plant. Meanwhile at  $t=100s$  and  $t=300s$ , we can see oscillations of pressure and flow dynamics due to change of main pump flow during connection.

## Case 2: Lost Circulation

In this case, the simulation is performed to study the adaptive observer in the case of loss circulation. The aim is to be able to accurately estimate the bottomhole pressure and adapts to the unknown parameter, that is the fluid loss rate. The MATLAB scripts and functions for this simulation is written in Appendix B. The depth of vertical well is 700m, and the flow rate of the main pump is 1000lpm. The simulation starts with normal drilling operation and normal main pump flow at 1000lpm. At  $t=150s$ , it is assumed that a highly permeable zone is drilled and as a result lost circulation occurs. The rate of fluid loss is gradually increase as the mud start to flow into the formation until it stables at some point. The numerical values used for the physical parameters are given in Table 5.1

**Table 5.1: Wellbore Parameters for Simulation of Loss Circulation**

<b>Parameter</b>	<b>Description</b>	<b>Value</b>	<b>Unit</b>
$\beta$	Bulk modulus	$2 \times 10^9$	$Pa$
$A_a$	Annulus cross sectional area	0.03	$m^2$
$A_d$	Drillstring cross sectional area	0.006	$m^2$
$F$	Friction factor	1	$kg/m^3$
$g$	Gravity constant	9.81	$m/s^2$
$\rho$	Mud density	1250	$kg/m^3$

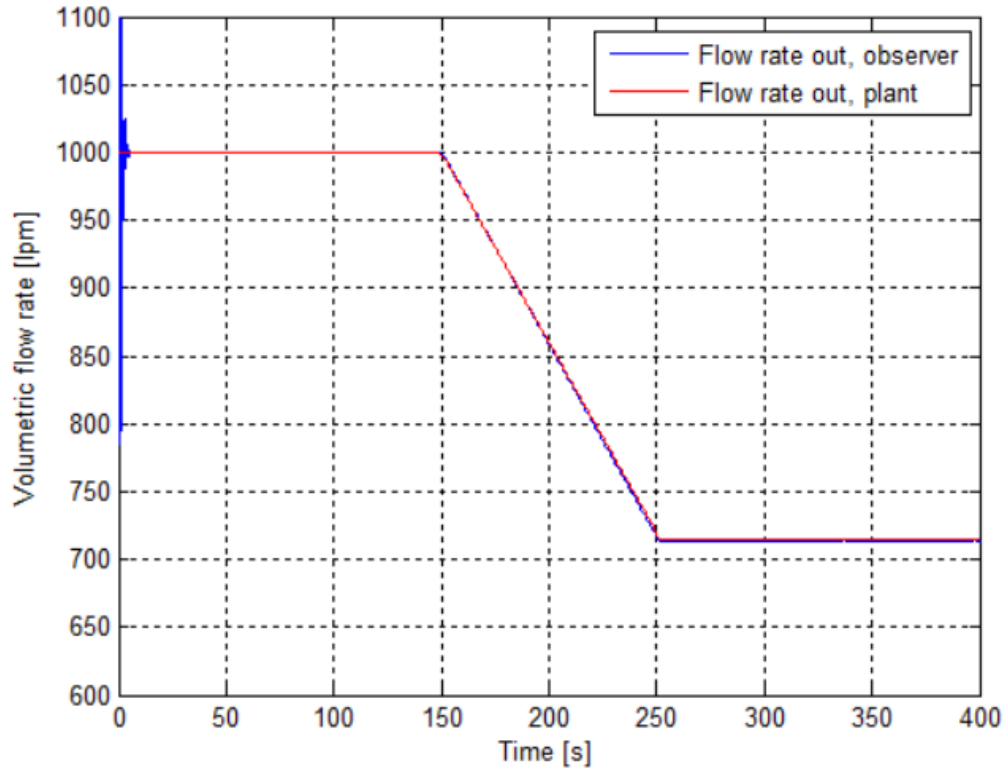


**Figure 5.5: Flowrate at the Outlet (Choke)**

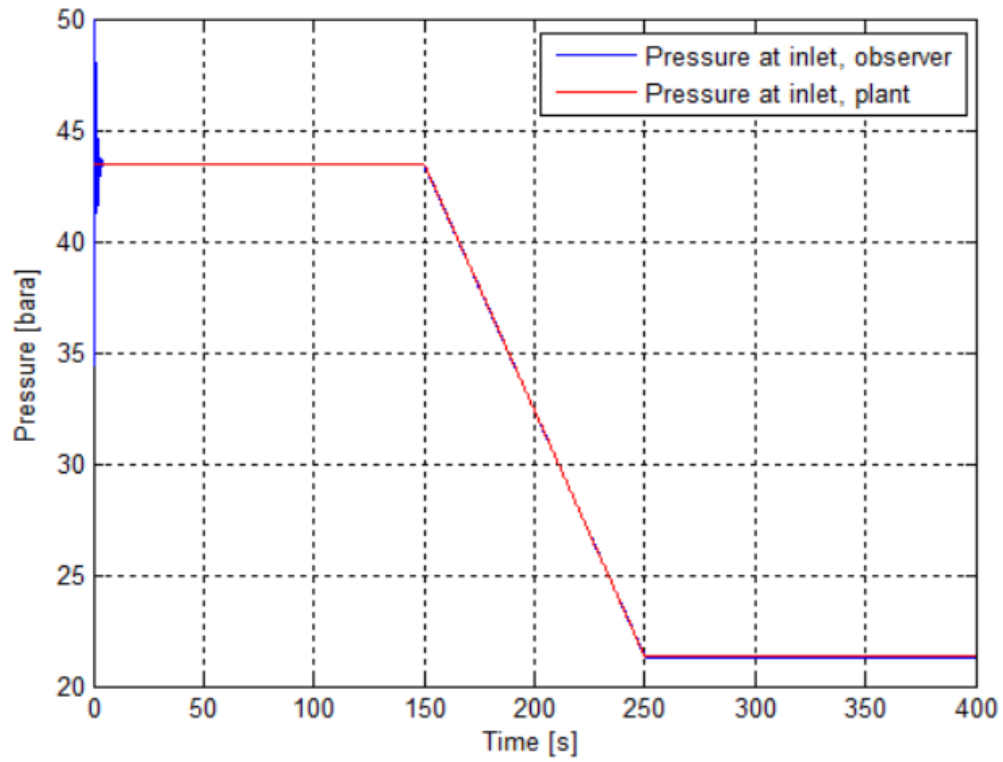


**Figure 5.6: Pressure at the Inlet (Bottomhole)**

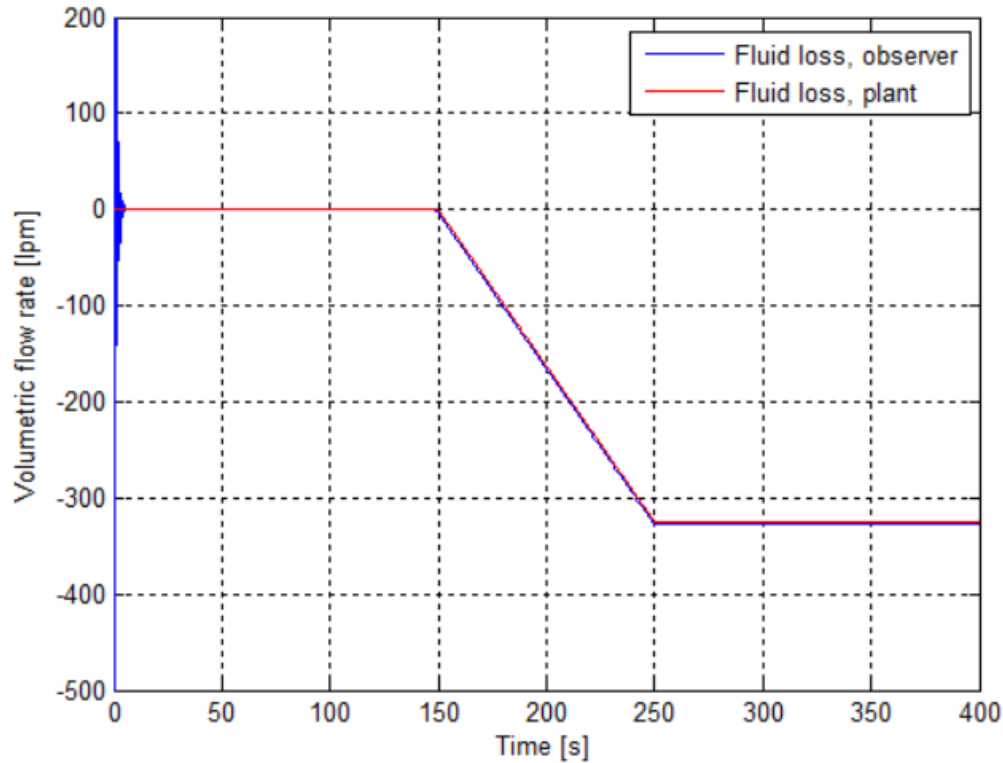


**Figure 5.7: Fluid Loss Estimation**

Figure 5.5 – 5.7 shows flow and pressure dynamics during loss circulation. The estimated and measured flowrate at the topside and downhole pressure can be seen from Figure 5.5 and Figure 5.6, respectively. Meanwhile Figure 5.7 shows the fluid loss during drilling operation. At  $t=150s$ , drilling encounter a highly permeable formation and as a result drilling fluid flow into the formation. Figure 5.5 shows that initially flowrate is maintained at 1000lpm. Due to the loss circulation at  $t=150s$ , the flowrate out of the hole is gradually decrease, and it affects the downhole pressure in Figure 5.6. Figure 5.7 shows the fluid loss due to high permeable zone. The fluid loss gradually increases to the point where the loss circulation stable at 320lpm. As the fluid loss stable at  $t=250s$ , the flowrate and the downhole pressure are going down to 720lpm and 22bara, respectively.

These simulations show that the adaptive observer design has been successfully implemented in order to provide state estimation such as flow dynamics and downhole pressure during drilling connection and lost circulation. The results show that the adaptive observer converges to the actual value and that the update law accurately estimates the unknown parameter, that is the fluid loss rate.

## 6. CONCLUSION AND FUTURE WORK

### 6.1 CONCLUSION

The main conclusion from this thesis is related to the adaptive observer design for linear hyperbolic system in MPD operation that is presented in Chapter 5.

- An adaptive observer that fulfills the main goals stated in Section 1.2 has been presented in Chapter 5. The adaptive observer is capable to accurately estimate the pressure and flow dynamics in the hydraulic system of MPD operations using only one measurement at the boundary (topside) and adapts to key unknown parameters such as fluid loss for an accurate downhole pressure estimation.
- The adaptive observer design is based on a backstepping method that have been successfully used for state and parameter estimation of many types of PDEs. It allows the design of the boundary observers that is exponentially stable at the origin guarantee the convergence of the state estimates. It also shows that the observer gain can be obtained by solving a first-order Goursat-type PDEs through a suitable infinite series of powers of partial derivatives in terms of special functions, such as Bessel functions and the generalized Marcum Q-functions of the first order.
- Simulation of the system dynamics produce state outputs that reflect the plant or measurement to a satisfactory degree. It shows that the observer can handle scenarios during drilling operation such as change in main pump flow during connection and change of hydraulic dynamics due to loss circulation. The result shows promising behavior of adaptive observer for hydraulic system in MPD, and it might offer wide range of application in MPD operation.

### 6.2 FUTURE WORK

Few suggestions for the future work, including:

- In this thesis, the hydraulic model is represented by a one-phase (liquid) incompressible flow model. In the future, we can consider a hydraulic model of the two-phase (gas-liquid) flow in the wellbore to be used for Underbalanced Drilling application or Kick / Well Control



scenarios. When linearized, the model takes the form of a first-order hyperbolic system as presented in this thesis. The uncertainty of the downhole conditions might result in uncertain boundary parameters in the linearized model. A boundary observer design involving more than two PDE states may be developed for this purpose in the future works.

- The controller design is not yet discussed in this thesis. It is important especially in the case of MPD operation to have a control law that regulates the downhole pressure to its set point. As the simplified hydraulic model has been transformed into  $2 \times 2$  linear hyperbolic system, the identified system model could serve as a necessary prerequisite to develop the controller design.

## REFERENCE

- Aadnoy, B., Cooper, I., Misca, S., Mitchell, R.F., Payne, M.L.** (2009). *Advanced Drilling and Well Technology*. SPE
- Aamo, O.M.** (2013). *Disturbance Rejection in 2 x 2 Linear Hyperbolic Systems*. IEEE Transaction on Automatic Control, 58(5), pp. 1095-1106.
- Anfinson, H.** (2013). *Disturbance Attenuation in Linear 2 x 2 Hyperbolic Systems with Application to the Heave Problem in Managed Pressure Drilling*. Master's Thesis, Department of Engineering Cybernetics. Norwegian University of Science and Technology.
- Azar, J.J., Samuel, R.** (2007). *Drilling Engineering*. Pennwell Corporation.
- Chrzanowski, W.S.** (2011). *Managed Pressure Drilling from Floaters: Feasibility Studies for Applying Managed Pressure Drilling from a Floater on the Skarv/Idun Field on the Norwegian Continental Shelf by PGNiF Norway AS*. Master's Thesis, University of Stavanger
- Godhavn, J.-M.** (2009). *Control Requirements for high-end automatic MPD Operations*. Amsterdam, Netherlands. SPE/IADC Drilling Conference and Exhibition. SPE/IADC 119442.
- Halliburton.** *Customer Guide to Managed Pressure Drilling*.  
<http://www.halliburton.com/public/ts/contents/Brochures/web/GBA-CustomerGuide.pdf>
- Hannegan, D.** (2006). *Case Studies – Offshore Managed Pressure Drilling*. San Antonio, Texas. San Antonio, Texas. SPE Annual Technical Conference and Exhibition. SPE 101855.
- Hannegan, D.** (2007). *Managed Pressure Drilling*. SPE 2006 – 2007 Distinguished Lecturer Series.
- Hannegan, D.** (2009). *Offshore Drilling Hazard Mitigation: Controlled Pressure Drilling Redefines What is Drillable*. Drilling Contractor Journal, 84-89.
- Hasan, A.** (2014). *Adaptive Boundary Control and Observer of Linear Hyperbolic Systems with Application to Managed Pressure Drilling*. San Antonio, Texas. Proceedings of the ASME 2014 Dynamic Systems and Control Conference
- Hasan, A.** (2015). *Adaptive Boundary Observer for Nonlinear Hyperbolic Systems: Design and Field Testing in Managed Pressure Drilling*. Chicago, Illinois. 2015 American Control Conference

- Hauge, E., Aamo, O.M., Godhavn, J.-M.** (2013). *Application of an Infinite Dimensional Observer for Drilling Systems Incorporating Kick and Loss Detection*. Zurich, Switzerland. In Proceedings of the European Control Conference.
- Kaasa, G.-O.** (2007). *A Simplified Dynamic Model of Drilling for Control*. StatoilHydro Research Centre Porsgrunn.
- Kaasa, G.-O., Starnes, Ø.N., Imsland, L., Aamo, O.M.** (2011). *Intelligent Estimation of Downhole Pressure Using a Simple Hydraulic Model*. Denver, Colorado. IADC/SPE Managed Pressure Drilling and Underbalanced Operations Conference and Exhibition. IADC/SPE 143097
- Mathworks.** *Documentation of MATLAB algorithm.*  
<http://se.mathworks.com/help/matlab/ref/ode23.html>
- Merritt, H. E.** (1967). *Hydraulic Control Systems*. John Wiley & Sons, Inc.
- Meglio, F.D., Bresch-Pietri, D., Aarsnes, U.** (2014). *An Adaptive Observer for Hyperbolic Systems with Application to Underbalanced Drilling*. Cape Town, South Africa. In Proceedings of the Ifac World Congress.
- Nauduri, S., Medley, G.H., Schubert, J.J.** (2009). *MPD: Beyond Narrow Pressure Windows*. San Antonio, Texas. IADC/SPE Managed Pressure Drilling and Underbalanced Operations Conference & Exhibition. IADC/SPE 122276.
- Nas, S., Torolde, J.S., Wuest, C.** (2009). *Offshore Managed Pressure Drilling Experiences in Asia Pacific*. Amsterdam, Netherland. SPE/IADC Drilling Conference and Exhibition. SPE 119875.
- Nygaard, G. H., Johannessen, E., Gravdal, J. E., Iversen, F.** (2007), *Automatic coordinated control of pump rates and choke valve for compensating pressure fluctuations during surge and swab operations*. Galveston, Texas. IADC/SPE Managed Pressure Drilling and Underbalanced Operations Conference and Exhibition. SPE 108344.
- Nygaard, G. H., Vefring, E.H., Fjelde, K.-K., Nævdal, G., Lorentzen, R.J., Mlyvaganam, S.** (2007), *Bottomhole Pressure Control During Drilling Operations in Gas Dominant Wells*. Houston, Texas. SPE/IADC Underbalanced Technology Conference and Exhibition. SPE 91578.
- Rehm, B., Schubert, J., Haghshenas, A., Paknejad, A.S., Hughes, J.** (2008). *Managed Pressure Drilling*. Houston, Texas. Gulf Drilling Series.
- Schlumberger.** (2011). *Managed Pressure Drilling Erases the Lines*. Oilfield Review.

- Slettebø, D.** (2015). *State and Parameter Identification Applied to Dual Gradient Drilling with Oil Based Mud*. Master's Thesis, Department of Engineering Cybernetics. Norwegian University of Science and Technology.
- Stamnes, Ø.N.** (2007). *Adaptive Observer for Bottom Hole Pressure During Drilling*. Master's Thesis, Department of Engineering Cybernetics. Norwegian University of Science and Technology.
- Stamnes, Ø.N., Zhou, J., Kaasa, G.-O., Aamo, O.M.** (2008). *Adaptive Observer Design for the Bottomhole Pressure of a Managed Pressure Drilling System*. Cancun, Mexico. 47<sup>th</sup> IEEE Conference on Decision and Control.
- Vazquez, R., Krstic, M., Coron, J.** (2011). *Backstepping boundary stabilization and state estimation of a 2 x 2 linear hyperbolic system*. Orlando, USA. 50<sup>th</sup> IEEE Conference on Decision and Control.
- Vazquez, R., Krstic, M.** (2013). *Marcum Q-functions and Explicit Kernels for Stabilization of 2 x 2 Linear Hyperbolic Systems with Constant Coefficients*. Firenze, Italy. 52<sup>th</sup> IEEE Conference on Decision and Control.
- Weatherford.** *Weatherford's Managed Pressure Drilling (MPD) Services*.  
<http://www.weatherford.com/doc/wft023747>
- White, F.** (2007). *Fluid Mechanics*. McGraw-Hill, New York.
- Zhou, J., Nygaard, G., Godhavn, J.-M., Breyholtz, Ø., Verfring, E.H.** (2010). *Adaptive Observer for Kick Detection and Switched Control for Bottomhole Pressure Regulation and Kick Attenuation during Managed Pressure Drilling*. Baltimore, USA. 2010 American Control Conference.

# NOMENCLATURE

## General

- Symbols are generally defined right after they appear in the text
- Only the most used symbols are listed in the following section
- Over-dots signify differentiation with respect to time

## Alphabet

$A$	Cross-sectional area
$a$	Speed of sound
$d_{in}$	Inner diameter of annular flow area
$d_{out}$	Outer diameter of annular flow area
$F_a$	Friction coefficient for the annulus
$F_b$	Friction coefficient for the bit
$F_d$	Friction coefficient for the drill string
$F_g$	Gravitational forces
$F_w$	Frictional forces between the fluid and the wall
$g$	Gravity
$h$	True vertical depth
$k_c$	Choke parameter
$M$	Integrated density per cross section
$p^{ij}$	Observer kernels
$p_c$	Annulus choke pressure
$p_p$	Rig pump pressure
$p_1, p_2$	Gain functions
$q_b$	Flowrate through the bit
$q_{bpp}$	Backpressure pump flow
$q_c$	Annulus choke flow
$q_p$	Rig pump flowrate
$q_{res}$	Flowrate from the reservoir

$t$	Time variable
$U$	Control input
$u, v$	State variables
$V$	Control volume
$V_a$	Annulus volume
$V_d$	Drillstring volume
$w$	Mass flow rate
$y$	Measurement
$z_c$	Choke opening

### **Symbols**

$\beta_a$	Effective bulk modulus for annulus
$\beta_d$	Effective bulk modulus for drill string
$\epsilon$	System parameter
$\rho_a$	Fluid density in annulus
$\rho_d$	Fluid density in drillstring
$\theta$	Inclination

### **Abbreviation**

AFP	Annular Frictional Pressure
BHA	Bottomhole Assembly
BHP	Bottom Hole Pressure
BOP	Blowout Preventer
BP	Back Pressure
CBHP	Constant Bottomhole Pressure
DGD	Dual Gradient Drilling
DSV	Drillstring Valve
ECD	Equivalent Circulating Density
ESD	Equivalent Static Density
HPHT	High Pressure High Temperature
HSE	Health, Safety, and Environment

IADC	International Association of Drilling Contractors
MPD	Managed Pressure Drilling
MW	Mud Weight
NPT	Non- Productive Time
NRV	Non-Return Valve
OBD	Overbalanced Drilling
ODE	Ordinary Differential Equation
PDE	Partial Differential Equation
PLC	Programmable Logic Control
PMCD	Pressurized Mud Cap Drilling
RBOP	Rotating Blowout Preventer
RCD	Rotating Control Device
RKB	Rotary Kelly Bushing
ROP	Rate of Penetration
TD	Target Depth
TVD	True Vertical Depth
UBD	Underbalanced Drilling

## APPENDIX A

### Main Script

```
close all;
clear variables;
clc;

beta=2e9;
La=2000;
Dd=0.088;
Da=0.2;
Ad=Dd^2/4*pi;
Aa=Da^2/4*pi-Ad;
rho=1250;
F=1;

q=-1;

a=0.5*La*F/sqrt(rho*beta);

eps1=1/La*sqrt(beta/rho);
eps2=eps1;

N=40;
dt=0.1;
Tspan=0:dt:400;
xspan=(0:N+1)/(N+1);

c1=-0.5*F/rho*exp(2*a*xspan);
c2=-0.5*F/rho*exp(-2*a*xspan);

%% compute output injection gains

% Exclude boundaries
xspan=xspan(2:N+1);
c1=c1(2:N+1);
c2=c2(2:N+1);

% flow rate from pump
qp=1/60; % 1000 lpm

% Initial conditions.
load init_u_v
y01=[u_init v_init];

[tt,yy] = ode23(@(t,x) hypsys(t,x,0,qp,eps1,eps2,q,c1,c2),Tspan,y01);

uu=yy(:,1:N);
vv=yy(:,N+1:2*N);
```



```

[q0,p0]=uv2qp(uu(:,1), vv(:,1), a,La, beta, rho, Aa, 0);
[qL,pL]=uv2qp(uu(:,N), vv(:,N), a, La, beta, rho, Aa, La);

%% plotting
print_results

```

### Function hypsys

```

function [dx]=hypsyst(t,x,uin,qp,eps1,eps2,q,c1,c2)

if t>100;
    qp=0;
end

if t>300;
    qp=1/60;
end

N=length(x)/2;
dx=1/(N+1);

u=x(1:N);
v=x(N+1:2*N);

v0=2*v(1)-v(2); % Interpolate v to boundary
u0=q*v0+qp;
v1=uin; % Input.
dudx=(u-[u0;u(1:N-1)])/dx;
dvdx=( [v(2:N);v1]-v)/dx;

dx=[-eps1*dudx+c1' .*v; ...
     eps2*dvdx+c2' .*u];

```

### Function uv2gp

```

function [ q,p ] = uv2gp( u,v,a,l,beta,rho,Aa,z )
%UV2QP Converts from u and v coordinates back to flow and pressure
% Detailed explanation goes here

if nargin<8
    z=linspace(0,l,numel(u));
end

q=u.*exp(-a/l*z)+v.*exp(a/l*z);
p=sqrt(beta*rho)/Aa*u.*exp(-a/l*z)-v.*exp(a/l*z)+rho*9.81*(1-z);

end

```

## Print result

```
close all;

[T,X]=meshgrid(Tspan,xspan);
T_end=Tspan(end);

%h_fig(1)=figure('Name', 'u');
%mesh(T,X,uu');
%xlabel('Time [s]');
%ylabel('x [-]');
%zlabel('u');
%xlim([0 T_end]);
% grid;

%h_fig(2)=figure('Name', 'v');
%mesh(T,X,vv');
%xlabel('Time [s]');
%ylabel('x [-]');
%zlabel('v');
%xlim([0 T_end]);
% grid;

h_fig(5)=figure('Name', 'flowrate_in');
ax(5:6)=plot(Tspan, q0*60e3);
grid;
xlabel('Time [s]');
ylabel('Volumetric flow rate [lpm]');
legend('Flow rate in, plant');
xlim([0 T_end]);

h_fig(6)=figure('Name', 'flowrate_out');
ax(7:8)=plot(Tspan, qL*60e3);
grid;
xlabel('Time [s]');
ylabel('Volumetric flow rate [lpm]');
legend('Flow rate out, plant');
xlim([0 T_end]);

h_fig(7)=figure('Name', 'pressure_in');
ax(9:10)=plot(Tspan, p0*1e-5);
grid;
xlabel('Time [s]');
ylabel('Pressure [bara]');
legend('Pressure at inlet, plant');
xlim([0 T_end]);

h_fig(8)=figure('Name', 'pressure_out');
ax(11:12)=plot(Tspan, pL*1e-5);
grid;
xlabel('Time [s]');
ylabel('Pressure [bara]');
legend('Pressure at outlet, plant');
xlim([0 T_end]);
```

## APPENDIX B

### Main Script

```
close all;
clear variables;
clc;

load q_c_m_sim.mat;
load q_dh_m_sim.mat;
load p_c_m_sim.mat;
load p_dh_m_sim.mat;
load q_lss_m_sim.mat;
load u_t.mat;

q_c_m_sim=smooth(q_c_m_sim,0.01,'rloess');

beta=2e9;
La=700;
Dd=0.1243;
Da=0.1548;
Ad=Dd^2/4*pi;
Aa=Da^2/4*pi-(Ad/0.93);
rho=1000;
F=100;
q=-1;
a=0.5*La*F/sqrt(rho*beta);

for i=1:length(q_c_m_sim);

u_1_m(i)=0.5*((q_c_m_sim(i)/60e3)+(Aa/sqrt(beta*rho))*(p_c_m_sim(i)/1e
-5))*exp(La*F/(2*sqrt(beta*rho)));
end

eps1=1/La*sqrt(beta/rho);
eps2=eps1;

N=40;
dt=0.1;
Tspan=0:dt:400;
xspan=(0:N+1)/(N+1);

c1=-0.5*F/rho*exp(2*a*xspan);
c2=-0.5*F/rho*exp(-2*a*xspan);

%% compute output injection gains

% Exclude boundaries
xspan=xspan(2:N+1);
c1=c1(2:N+1);
```

```

c2=c2(2:N+1);

% flow rate from pump
qp=1/60; % 1000 lpm

% Initial conditions.
load init_u_v
y01=[u_init v_init];

[tt,yy] = ode23(@(t,x)
hypsyst(t,x,0,qp,eps1,eps2,q,c1,c2,u_1_m,u_t),Tspan,y01);

uu=yy(:,1:N);
vv=yy(:,N+1:2*N);

[q0,p0]=uv2qp(uu(:,1), vv(:,1), a,La, beta, rho, Aa, 0);
[qL,pL]=uv2qp(uu(:,N), vv(:,N), a, La, beta, rho, Aa, La);

[theta,pH]=uv2qp(3.5*(u_1_m'-uu(:,N)), vv(:,N), a, La, beta, rho, Aa,
La);

%% plotting
print_results

```

### Function hypsys

```

function [dx]=hypsyst(t,x,uin,qp,eps1,eps2,q,c1,c2,u_1_m,u_t)

u_1_m = interp1(u_t,u_1_m,t);

N=length(x)/2;
dx=1/(N+1);

u=x(1:N);
v=x(N+1:2*N);

v0=2*v(1)-v(2); % Interpolate v to boundary
u0=q*v0+qp;
v1=uin; % Input.
dudx=(u-[u0;u(1:N-1)])/dx;
dvdx=( [v(2:N);v1]-v)/dx;

dx=[-eps1*dudx+c1'.*v+0.4*(u_1_m-u);...%0.4
eps2*dvdx+c2'.*u-5*(u_1_m-u)]; %5

```

### Function uv2gp

```

function [ q,p ] = uv2gp( u,v,a,l,beta,rho,Aa,z )
%UV2QP Converts from u and v coordinates back to flow and pressure
% Detailed explanation goes here

```

```

if nargin<8
    z=linspace(0,1,numel(u));
end

q=u.*exp(-a/l*z)+v.*exp(a/l*z);
p=sqrt(beta*rho)/Aa*(u.*exp(-a/l*z)-
v.*exp(a/l*z))+rho*sin(pi/360)*9.81*(1-z);
end

```

## Print result

```
close all;
```

```
[T,X]=meshgrid(Tspan,xspan);
T_end=Tspan(end);
```

```

%h_fig(1)=figure('Name', 'u');
%mesh(T,X,uu');
%xlabel('Time [s]');
%ylabel('x [-]');
%zlabel('u');
%xlim([0 T_end]);
% grid;
%

```

```

%h_fig(2)=figure('Name', 'v');
%mesh(T,X,vv');
%xlabel('Time [s]');
%ylabel('x [-]');
%zlabel('v');
%xlim([0 T_end]);
% grid;
%

```

```

%h_fig(5)=figure('Name', 'flowrate_in');
%ax(5:6)=plot(Tspan, q0*60e3);
%grid;
%xlabel('Time [s]');
%ylabel('Volumetric flow rate [lpm]');
%legend('Flow rate in, plant');
%xlim([0 T_end]);
%

```

```

h_fig(6)=figure('Name', 'Top side flow rate');
ax(7:8)=plot(Tspan, qL*60e3);hold
on;plot(u_t',smooth(smooth(smooth(smooth(q_c_m_sim))))', 'r');
grid;
xlabel('Time [s]');
ylabel('Volumetric flow rate [lpm]');
legend('Flow rate out, observer', 'Flow rate out, plant')
xlim([0 T_end]);
ylim([600 1100]);
%

```

```

h_fig(7)=figure('Name', 'Downhole pressure');
ax(9:10)=plot(Tspan, smooth(smooth(smooth(p0)))*1e-5);hold
on;plot(u_t',p_dh_m_sim', 'r');
%

```

```

grid;
xlabel('Time [s]');
ylabel('Pressure [bara]')
legend('Pressure at inlet, observer','Pressure at inlet, plant');
xlim([0 T_end]);
ylim([20 50]);

h_fig(8)=figure('Name', 'Fluid loss');
ax(9:10)=plot(Tspan, smooth(smooth(smooth(theta)))*60e3);hold on;plot(u_t',-
q_lss_m_sim','r');
grid;
xlabel('Time [s]');
ylabel('Volumetric flow rate [lpm]')
legend('Fluid loss, observer','Fluid loss, plant');
xlim([0 T_end]);
ylim([-500 200]);

%h_fig(8)=figure('Name', 'pressure_out');
%ax(11:12)=plot(Tspan, pL*1e-5);
%hold on;
%ax(13:14)=plot(Tspan, smooth(p0*1e-5),'r');
%grid;
%xlabel('Time [s]');
%ylabel('Pressure [bara]')
%legend('Pressure at outlet, plant')
%xlim([0 T_end]);
%ylim([20 45]);

```